A high-throughput screening platform for discovering bacterial species and small molecules that modify animal physiology

Kelsie M. Nauta[1], Darrick Gates[1], Marco Mechan-Llontop[1], Xiao Wang[1], Kim Nguyen[1], Christine N. Isaguirre[2], Megan Genjdar[2], Ryan D. Sheldon[2], Nicholas O. Burton[1]*

[1]Van Andel Research Institute, Department of Metabolism and Nutritional Programing, Grand Rapids, MI, 49503, USA

[2]Van Andel Research Institute, Mass Spectrometry Core, Grand Rapids, MI, 49503, USA

*Corresponding author: Nick.Burton@vai.org

Keywords

C. elegans, microbiome, insulin, polyamines, N1-aminopropylagmatine, *Bacillus subtilis*, mitochondria, *speB*, *daf-2, hsp-6, catp-5*

Abstract

The gut microbiome has been proposed to influence many aspects of animal development and physiology. However, both the specific bacterial species and the molecular mechanisms by which bacteria exert these effects are unknown in most cases. Here, we established a high throughput screening platform using the model animal *Caenorhabditis elegans* for identifying bacterial species and mechanisms that influence animal development and physiology. From our initial screens we found that many *Bacillus* species can restore normal animal development to insulin signaling mutant animals that otherwise do not develop to adulthood. To determine how *Bacilli* influence animal development we screened a complete non-essential gene knockout library of *Bacillus subtilis* for mutants that no longer restored development to adulthood. We found the *Bacillus* gene *speB* is required for animal development. In the absence of *speB*, *B. subtilis* produces excess N1-aminopropylagmatine. This polyamine is taken up by animal intestinal cells via the polyamine transporter CATP-5. When this molecule is taken up in sufficient quantities it inhibits animal mitochondrial function and causes diverse species of animals to arrest their development. To our knowledge, these are the first observations that *B. subtilis* can produce N1-aminopropylagmatine and that polyamines produced by intestinal microbiome species can antagonize animal development and mitochondrial function. Given that *Bacilli* species are regularly isolated from animal intestinal microbiomes, including from humans, we propose that altered polyamine production from intestinal *Bacilli* is likely to also influence animal development and metabolism in other species and potentially even contribute developmental and metabolic pathologies in humans. In addition, our findings demonstrate that *C. elegans* can be used as a model animal to conduct high throughput screens for bacterial species and bioactive molecules that alter animal physiology.

Introduction

The 1929 discovery of penicillin revolutionized modern medicine because it not only demonstrated that small molecules could be harnessed as antibiotics to treat bacterial infections, but that antibiotics naturally occur in the environment (1,2). This discovery, while transformative, was initially accidental. A few years later a former graduate student of Selman Waksman, Rene Dubos, would isolate the antibiotic tyrothricin from the soil bacterium *Brevibacillus brevis* (3,4). Collectively, these discoveries led Waksman to hypothesize that molecules that antagonize the growth of other bacteria could be deliberately and systematically isolated by screening soil microbes. The premise for this hypothesis largely derived from the idea that soil, which contains tens of thousands of species of bacteria per gram (5,6), was a highly competitive environment which would promote the evolution of such molecules for certain species of bacteria to gain a competitive advantage. As proof-of-principle Waksman would develop what became known as the Waksman platform for the systematic screening of soil bacteria for antibiotic properties against pathogenic bacteria (7). By screening >10,000 different bacterial isolates, Waksman and his associates would go on to discover many new classes of antibiotics we still use clinically today, including streptomycin (7). The ability to run high throughput screens for antibiotic molecules from soil led to what is now known as the “golden age of antibiotics” (8).

While the Waksman platform was highly successful in identifying molecules that antagonize the growth of other bacteria, by its nature it could not identify any other type of molecule bacteria might make to interact with other forms of life in their environment. For example, nearly all soil on earth is inhabited by bacterivorous nematodes and protists (6,9). These eukaryotes are predators of soil microbes, and in the case of nematodes, also represent a potential new niche

for bacteria to live in and colonize the intestinal microbiome of these animals (10). For the same reasons that the diversity of life in soil drove the evolution of antibiotics, we hypothesize that similar competitive pressures should also drive the evolution of molecules that target eukaryotic and animal physiology.

Discoveries of antibiotics by Fleming and Dubos gave credence to the idea that environmental microorganisms harbor molecules that are clinically useful for targeting pathogenic bacteria. Similarly, we already have evidence that soil microbes produce clinically relevant small molecules that target eukaryotic/animal physiology. For example, the discovery of avermectin from soil bacteria led to one of the gold standard treatments for parasites (ivermectin) (11). Similarly, rapamycin has been isolated from soil bacteria and is now used clinically as an immunosuppressant (12). Nonetheless, far fewer molecules produced by soil bacteria that target animal physiology have been discovered when compared to antibiotics. We hypothesize that this is not because such molecules and mechanisms do not exist or are not common, but rather because there currently exists no equivalent to the Waksman platform that can systematically screen soil bacteria for molecules/mechanisms that target animal physiology. The reasons for this are varied but include the fact that most animals already harbor their own microbiomes that are resistant to colonization by external bacteria (13). Thus, bacteria cannot be systematically screened one by one for effects on animal physiology without germ free animals which are costly to maintain in most cases (14,15).

Here, we report the development of a high throughput screening platform using the model animal *Caenorhabditis elegans* to screen for bacterial mechanisms and molecules that influence animal physiology. As proof-of-principle we screened >5,000 wild bacterial isolates for species

that could modify the developmental trajectory of insulin signaling mutant animals. We discovered that many *Bacillus* species are capable of restoring normal animal development in insulin signaling mutants that otherwise arrest development as dauer-stage animals (16). Furthermore, by screening a complete nonessential gene knockout library of *Bacillus subtilis* (*Bs*) we found that a polyamine produced by this species, N1-aminopropylagmatine, antagonizes the development of diverse species of nematodes including *C. elegans* and *Pristonchus pacificus* (17). Lastly, we report that the ability of N1-aminoprophylagmatine to antagonize animal development depends on the polyamine transporter CATP-5 in animals and correlates with the activation of the mitochondrial unfolded protein response. To our knowledge, these findings represent the first observation that polyamines produced by bacteria can antagonize animal development and demonstrate that *C. elegans* can be used as a model animal to run high throughput screens for bacterial species and small molecules that modify animal physiology.

Results

Bacillus species promote animal development

To identify novel bacterial mechanisms that influence animal development and physiology we developed a high-throughput platform for screening the effects of individual bacterial isolates on animals using the model animal *Caenorhabditis elegans* (Fig. 1A). To enrich potentially beneficial or commensal bacteria, as opposed to toxic or pathogenic bacteria, we initially developed our platform to screen for bacterial species that could restore normal animal development in mutant animals that harbor a mutation in the *C. elegans* insulin receptor ortholog *daf-2*. Briefly, when *daf-2(e1368)* mutant animals are fed a normal laboratory diet of *E.*

coli OP50 at elevated temperatures (26 °C), they arrest development in a metabolically inert state called dauer (16). We hypothesized that bacteria might harbor mechanisms that could promote animal insulin signaling because in *C. elegans* insulin signaling status can modify which bacteria are capable of colonizing the animal's intestine (18,19). Furthermore, we hypothesized that while *daf-2(e1368)* mutants would arrest in dauer when fed most soil microbes, microbes harboring mechanisms that could promote animal insulin signaling would enable *daf-2(e1368)* mutants to fully develop to adulthood.

As proof-of-principle, we first isolated a library of 4,000 bacterial isolates from 7 compost or soil samples in Michigan, USA. We then arrayed ~200 germ-free *daf-2(e1368)* mutant embryos on each of these 5,000 bacterial isolates in 12-well plates and placed them at 26 °C for 5 days (Fig. 1A). From this screen, we identified a strain of *Bacillus velezensis (NOBb03)* that restored the ability of *daf-2* mutant animals to develop to adulthood (Fig. 1B). To determine if this capability was conserved amongst *Bacilli*, we tested closely and distantly related species (Fig. 1B, SFig. 1). We found that suppression of *daf-2(e1368)* is conserved in many *Bacilli*, including the model species *Bacillus subtilis* (*Bs*). Since genetic tools exist to study *B. subtilis*, we used *B. subtilis* to model the effects of *Bacillus* species on animal development and physiology (17).

Mutations in the TGF-β signaling pathway also cause *C. elegans* to arrest as dauers at elevated temperatures. This is because the loss of either insulin signaling or TGF-β signaling results in the activation of the hormone receptor DAF-12 which drives dauer developmental arrest (20). To test if the effects of *Bacillus* species were specific to the loss of animal insulin signaling or if *Bacilli* might generally promote animal development or antagonize dauer developmental arrest, we also placed a temperature sensitive TGF-β signaling mutant, *daf-1*(*m40*) on *E. coli* OP50

and *B. subtilis* at 26 °C for 5 days. We found that *B. subtilis* was not sufficient to promote development to adulthood for TGF- β mutants (Fig. 1C-E). The failure of *B. subtilis* to suppress dauer arrest in TGF- β mutants (*daf-1*) could be because *B. subtilis* specifically affects the phenotype of insulin signaling mutants or because *daf-1* mutations are not suppressible by bacteria due to intrinsic differences between the *daf-1* and *daf-2* mutations. To test this possibility, we screened our bacterial isolate library for bacteria that could suppress the dauer arrest phenotype of *daf-1(m40)* [TGF-β receptor] mutants. From this screen we found that *Pseudomonas lurida* strains, including the *C. elegans* microbiome strain MYb11 (21) could suppress the dauer arrest phenotype of TGF-β mutants (*daf-1*) but not of Insulin receptor (*daf-2*) mutants (Fig. 1C-E). We conclude that *Bacilli* species specifically suppress the dauer arrest phenotype of insulin signaling mutants. Furthermore, these findings demonstrate that our high-throughput screening platform can identify bacterial species that restore normal development in mutant animal models of clinically relevant signaling pathways (Insulin and TGF-β signaling).

speB is required in _B. subtilis_ to promote animal development

To identify *B. subtilis* genes that are required to promote development of *daf-2(e1368)* mutants, we arrayed germ-free *daf-2(e1368)* mutant embryos on a complete *B. subtilis* non-essential gene knockout library (Fig. 2A) (17). From a screen of 3,984 mutant *B. subtilis* isolates, we identified only a single *B. subtilis* gene, *speB*, that was required for *daf-2(e1368)* mutants to develop to adulthood (Fig 2B, Fig. 2C). SpeB encodes an agmatinase which plays an intermediate role in the synthesis of spermidine (22,23). We confirmed that *speB* is required for *daf-2(e1368)* mutants to develop to adulthood by rescuing this mutant effect with a wild-type copy of *speB* (Fig. 3B, 3C). To test if *speB* is also required for the development of wild-type

animals or if this effect is specific to *daf-2(e1368)* mutants, we grew wild-type animals on *B. subtilis* and *B. subtilis* Δ*speB*. We found that wild-type animals also failed to properly develop to adulthood when fed *B. subtilis* Δ*speB* (Fig. 2D, 2E). Collectively, we conclude that *speB* is required in *B. subtilis* to promote *C. elegans* development to adulthood.

B. subtilis **produces N1-aminopropylagmatine to antagonize animal development**

To determine how a diet of *B. subtilis* Δ*speB* antagonizes animal development, we mutagenized wild-type *C. elegans* and screened for mutant animals that could develop to adulthood when feeding on *B. subtilis* Δ*speB.* We isolated 10 lines of mutant animals that developed to adulthood even when fed *B. subtilis* Δ*speB* (Fig. 3A, Fig. 3B, SFig. 2, Table 1). We found all the isolated mutant lines harbored predicted loss-of-function mutations in the *catp-5* polyamine transporter (Fig. 3C). CATP-5 was previously reported to import polyamines into the intestinal epithelium (24). These findings suggest that *B. subtilis* Δ*speB* likely makes excess amounts of a polyamine molecule that is imported by CATP-5 into animal intestinal cells and inhibits animal development.

SpeB is part of a pathway, together with SpeA and SpeE, that converts arginine to spermidine (Fig. 4A). To determine if animals are unable to develop to adulthood on *speB* mutant *B. subtilis* because they require spermidine from their diet and SpeB is required to make spermidine, we tested if the deletion of *speA* or *speE* also caused animals to arrest their development. We found that deletion of *speA* and *speE* did not alter WT animal development (Fig. 4B, Fig. 4C, Fig. 4D) or suppress dauer in *daf-2*(*e1368*) animals (SFig. 2). Since *speA* is known to convert L-arginine into agmatine, we generated a double Δ*speA* Δ*speB* deletion strain to test if aberrant

accumulation of agmatine might inhibit animal development. We found deletion of *speA* in the Δ*speB* background rescued *C. elegans* development (Fig. 4C, 4D). We confirmed this phenotype by complementing Δ*speA* Δ*speB* with *speA* (Fig. 4C, 4D). Surprisingly, we found that knocking out the *speEB* operon does not phenocopy Δ*speB* (Fig. 4C, Fig. 4D). We confirmed this result by complementing Δ*speEB* with *speE* and found the strain no longer promoted animal development (Fig. 4C, 4D). We conclude that the deletion of *speB*, but not other genes in the spermidine synthesis pathway, antagonizes animal development and that this effect is dependent on both *speA* and *speE* activity. These unexpected findings suggest that the predicted polyamine synthesis pathway in *B. subtilis* is not complete and that SpeA and SpeE activity are capable of generating a polyamine that builds up in the absence of SpeB and antagonizes animal development when animals uptake this polyamine via the polyamine transporter CATP-5.

We hypothesized that *B. subtilis speB* mutants were producing an aberrant polyamine that antagonized animal development. To test this, we evaluated the polyamine profile in *B. subtilis ΔspeA*, *ΔspeB*, *ΔspeEB*, *ΔspeE*, *ΔspeB; ΔspeA*, and WT cultures. Polyamines are not well retained or ionized in typical LC-MS metabolomics approaches. So, to do this we generated carbamyl derivatives of metabolite extracts and performed untargeted metabolomics. Using this approach, we detected 2641 blank- and peak quality-filtered LC-MS features. Differential abundance analysis revealed a consistent feature, 388.29207 m/z at retention time of 3.781min, was the most significantly increased compound in *ΔspeB* cells versus the other polyamine synthesis mutants (Figure 5A). Evaluation of extracted ion chromatograms (EIC) indicated that this compound was only detectable in the *ΔspeB* cells (Figure 5B). Using accurate mass MS1 measurements, we found three possible chemical formulae within 5ppm (Figure 5C). Of these, only one contained oxygen atoms, of which there are two per carbamyl derivative (C5H9O2;

Figure 5C). From this we deduced that the unknown compound contained two carbamyl-derivatized sites, and subtraction of 2x($C_5H_9O_2$) from the predicted chemical formula of the unknown ($C_{18}H_{37}N_5O_4$) yielded a parent compound formula of $C_8H_{21}N_5$. This is consistent with the non-canonical polyamine N1-aminopropylagmatine (N1-APA; (Figure 5D). To confirm this putative identification, we spiked synthetic standard to *ΔspeB* media and observed an increased in the 388.2921 EIC over unspiked *ΔspeB* controls (Figure 5E). MS2 fragmentation spectra of the endogenous unknown and the synthetic standard further confirmed the identity of the *ΔspeB* specific polyamine as N1APA (Figure 5F).

In the extremophile *Thermus thermophilus*, SpeE has been shown to alternatively convert agmatine into N1-aminopropylagmatine which is then converted into spermidine by SpeB (Fig. 5G) (25). To our knowledge, *T. thermophilus* is the only known bacteria to utilize this alternative spermidine synthesis pathway. We hypothesized that *B. subtilis* is also capable of producing N1-aminopropylagmatine via SpeE activity and that when *speB* is deleted, N1-aminopropylagamtine accumulates and causes animals to arrest their development. We then tested if N1-aminopropylagamatine was sufficient to inhibit animal development. We grew *C. elegans* on a diet of WT *B. subtilis* on media containing added exogenous N1-aminopropylagmatine. We found exogenous N1-aminopropylagmatine was sufficient to inhibit animal development (Fig. 5H, SFig. 4A). We also found the addition of exogenous spermidine to the media is sufficient to suppress the effects of exogenous N1-aminopropylagamine (SFig. 4B) or *B. subtilis* Δ*speB* (SFig. 4C). We conclude that N1-aminotpropylagmatine production by *B. subtilis* antagonizes animal development, possibly by disrupting the normal function of spermidine.

N1-aminopropylagmatine causes mitochondrial stress in animals

To determine how N1-aminopropylagmatine antagonizes animal development, we screened 12 *C. elegans* GFP stress reporters on a diet of either *B. subtilis* or *B. subtilis* Δ*speB* (Table 2). We found that GFP reporters for *hsp-6* and *irg-1* were both substantially increased when animals were fed Δ*speB* mutant *B. subtilis* when compared to wild-type *B. subtilis* (Fig. 6A) or compared to other polyamine synthesis mutants (SFig. 5). *hsp-6* expression is part of the mitochondrial unfolded protein response and is activated in response to mitochondrial stress. *irg-1* was originally used as a reporter for bacterial infections, but later it was found that this reporter is also activated in response to mitochondrial stress (26). Thus, the activation of both *hsp-6* and *irg-1* is consistent with animals experiencing mitochondrial stress. This activation is reversed when a wild-type copy of *speB* was restored to the *B. subtilis* genome. Importantly, we did not observe a difference in level of fluorescence for the other nine reporters that were tested: *nlp-29, clec-60, gcs-1, hsp-60, hsp-16.2, gst-4, hsp-4, sod-3, bvIs5* (Table 2). The activation of the mitochondrial unfolded protein response is likely not due to general proteostasis stress because we did not observe activation of *hsp*-4::GFP which is activated as part of the endoplasmic reticulum unfolded protein response (SFig. 6, Table 2). We conclude that N1-aminopropylagmatine activates the *C. elegans* mitochondrial unfolded protein response, likely by causing mitochondrial stress.

The effects of N1-aminopropylagmatine could be specific to *C. elegans* or could generally antagonize animal development and mitochondrial function across species. To test this, we exposed the nematode *Pristionchus pacificus* to wild-type and Δ*speB B. subtilis* (Fig. 6B). *P. pacificus* and *C. elegans* shared a last common ancestor approximately 100 million years ago

(27,28). We found that Δ*speB B. subtilis* antagonized the development of *P. pacificus* and led to a >90% reduction animal fertility (Fig. 6C). We conclude that N1-aminiopropylagmatine broadly affects animal development and physiology and that this effect is not specific to *C. elegans.*

Discussion

A platform for identifying bacterial species and genes that modify animal physiology

C. elegans is gaining popularity as a model animal to study host-microbe interaction due, in part, to the ease of collecting numerous germ-free animals at scale (19,21,29–36). Our findings demonstrate that *C. elegans* can be used as a screening platform to identify both novel species of bacteria and novel metabolites that influence animal physiology. At the throughput described here we were able to screen >2,500 bacterial isolates per week. This throughput is not substantially different from the throughput of the Waksman platform which successfully identified numerous antibiotics produced by soil bacteria. Furthermore, as was the case for both antibiotics and previously discovered small molecules produced by soil bacteria that target eukaryotes/animals (rapamycin, avermectin), we found that N1-amniopropylagmatine elicits similar changes in animal physiology across distantly related species. We hypothesize that most bacterially produced molecules that target animals are likely to work on diverse species. This is because if natural selection is to favor the evolution of such small molecules, then it stands to reason that they would need to target highly conserved proteins, or their targets might quickly evolve resistance to such molecules. Furthermore, for bacteria to generate molecules that modify or target animal physiology, again like rapamycin and avermectin, they need to work at low concentrations, be able to cross membranes, and not generally cause toxicity to the bacteria itself. For these reasons, we believe that a platform that screens bacteria for novel

bioactive molecules that target animals is likely to overcome many of the challenges that normally face small molecules identified by screening small molecule libraries. Here, we selected bacteria as hits from our screen based on their ability to modify the development of insulin resistant mutant animals. However, in the future, we believe that this platform could be adapted to screen for bacteria that modify the physiology of diverse other mutant models of human disease including changes in TGF-β signaling (as demonstrated by our findings that *P. lurida* can suppress dauer development in TGF-β signaling mutants (Fig. 1E)) and TOR signaling.

SpeE can produce N1-APA in *Bacillus subtilis*

Previous work found that in the extremophile *Thermus thermophilus* SpeE can convert agmatine into N1-aminopropylagamitine. *T. thermophilus* SpeB subsequently converts N1-aminopropylagamtine into spermidine (Fig 4A). We provide evidence here that, while phylogenetically distinct from *T. thermophilus*, *B. subtilis* SpeE can also convert agmatine into N1-aminopropylagamtine as part of the process that leads to spermidine synthesis. Spermidine influences many physiological processes such as autophagy and aging, protein synthesis, cation transport, and mitochondrial function and biogenesis (37). Previous work suggested that polyamine analogs, such as norspermidine, can antagonize animal development and physiology, possibly by interfering with the normal role of spermidine (24). However, these previous studies hypothesized that polyamine analogs might be toxic due to interfering with the function of RNA or other nucleic acid processes. Here, we found that N1-aminopropylagmatine specifically causes activation of the mitochondrial unfolded protein response. We thus hypothesize that high concentrations of N1-aminopropylagmatine result in loss of *C. elegans* development by causing mitochondrial dysfunction (See model: Fig. 7). If N1-aminopropylagmatine generally interfered with the function of all RNAs, due to the positive

charge nature binding to negatively charged nucleic acids, then we would not expect it to specifically cause mitochondrial stress. Future studies will likely be critical in determining why N1-aminopropylagmatine specifically causes mitochondrial stress and if this phenomenon is due to sterically interfering with a normal function of spermidine in mitochondria.

T. thermophilus and *B. subtilis* are very distantly related. Given our findings here and the distant evolutionary relationship between these two species, it is likely that other diverse Gram-positive bacteria are also capable of producing N1-aminopropylagmatine. Under normal conditions, it does not appear that *B. subtilis* produces sufficient N1-aminopropylagmatine to cause animals to arrest their development and we in fact found that *B. subtilis* promotes the development of *daf-2* mutant animals. However, in other contexts, such as in *speB* mutant isolates, they did produce enough N1-aminopropylagmatine to antagonize animal development. Collectively, given our findings, we hypothesize that it is possible there are contexts, either environmentally or due to colonization by mutant bacteria, that intestinal bacteria present in humans also produce excess N1-aminopropylagmatine, either by *Bacilli* or other Gram-positive bacteria. If true, then our findings suggest that such N1-aminopropylagmatine might cause mitochondrial stress in humans and contribute to human pathologies. Future studies will be critical in determining if N1-aminopropylagmatine abundance correlates with any specific human pathologies, but our studies demonstrate the usefulness of our *C. elegans* screening platform to identify specific bacterial metabolites that modify animal physiology and provide a candidate molecule for further investigation.

Bacilli* suppress insulin resistance in *C. elegans.

We identified several related species of *Bacillus* that allow *daf-2* mutant animals to develop to adulthood even though the same mutants exclusively arrested development as dauers when feeding on their standard laboratory diet of *E. coli* OP50. Surprisingly, every single knockout from a complete nonessential gene knockout library of *B. subtilis* was still capable of restoring development to adulthood of *daf-2* mutants except *speB* mutants. Given that *speB* mutants produce excess N1-aminopropylagmatine which directly antagonizes animal development, it is likely that this effect is separate from the ability of *Bacilli* to restore development to *daf-2* mutants. Thus, it remains unknown how *Bacillus* species mediate this effect on *daf-2* mutants. One possibility is that there is a redundant mechanism that mediates this effect such that no individual gene in *B. subtilis* is required for this effect. An alternative option is that it depends on an essential gene in *B. subtilis* that was not part of the nonessential knockout library. Future studies will be critical in determining how and why *Bacillus* species can restore normal development to *daf-2* mutant animals. However, we note that most wild bacterial isolates from our screen were not capable of restoring development to *daf-2* mutants. Thus, we suspect that this mechanism is due to an active process in *Bacillus* species and not due to some common process present in all bacteria or due to any actively damaging process present in the control *E. coli* OP50 isolate that has long been used as a food source for laboratory *C. elegans.*

Acknowledgements

We would like to acknowledge Craig Ellermeier for sharing *Bacillus* strains and plasmids. Microbial strains used in this work were provided by the USDA-ARS Culture Collection (NRRL). This research was supported in part by the Van Andel Institute Mass Spectrometry Core (Grand Rapids, MI). We thank D. Chandler for helpful comments on the manuscript text, the *Caenorhabditis* Genetics Stock Center (funded by the NIH National Center for Research Resources) and National BioResource Project (NRBP) for *C. elegans* strains, and WormBase

as a repository of *C. elegans* data. This work was supported by funds from the VAI MeNu research grant program and NIH grant DP2DK139569.

Declarations of Interest

The authors declare that they have no competing interests.

Author Contributions

K. Nauta, D. Gates, and N. Burton formulated the project. K. Nauta, D. Gates, M. Mechan, X. Wang performed the experiments. K. Nguyen maintained *C. elegans* strains. C. Isaguirre, M. Genjdar, and R. Sheldon performed mass spectrometry experiments. K. Nauta, R. Sheldon, and N. Burton wrote the manuscript.

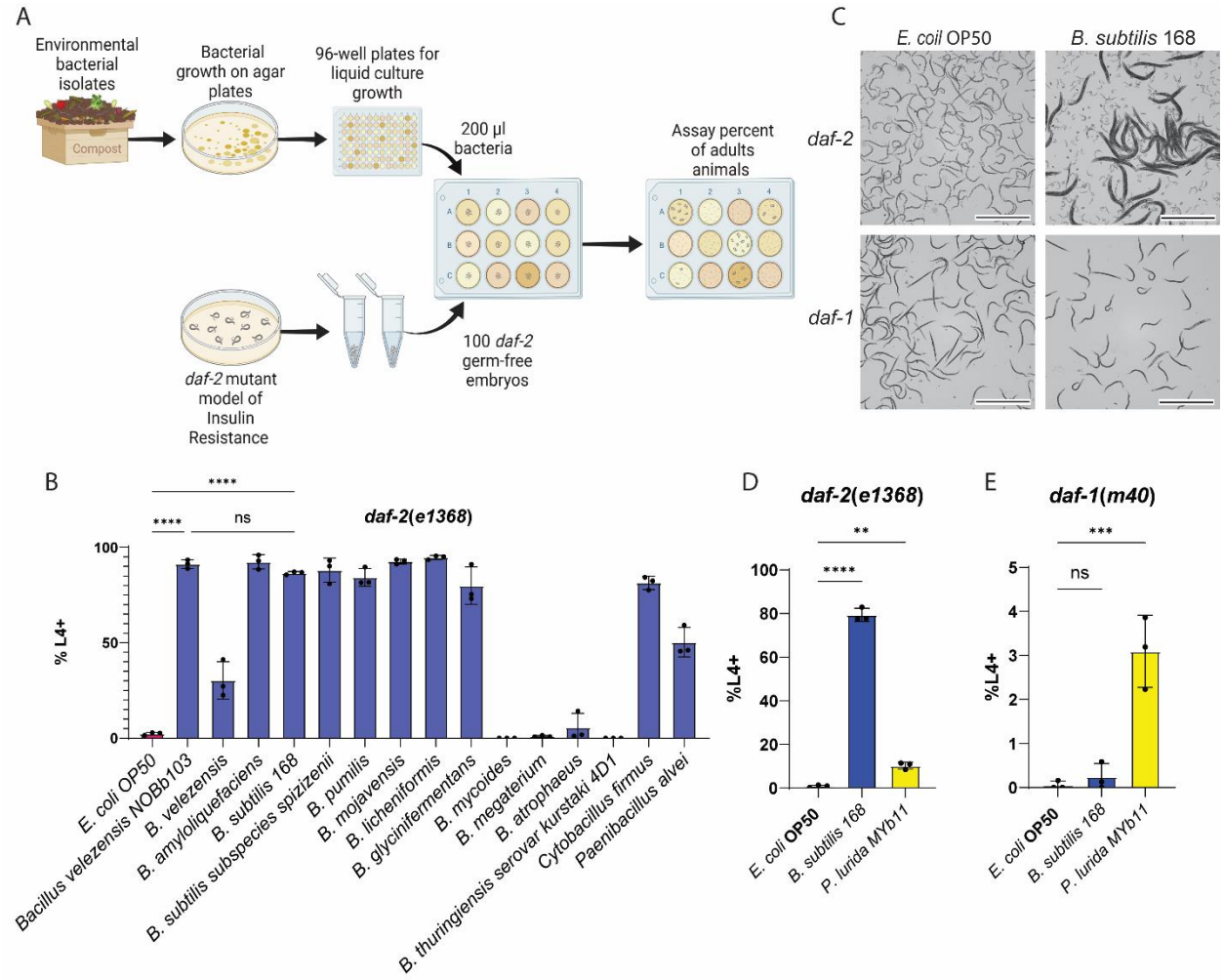

Figure 1: Screen of wild bacterial isolates and identification of *Bacillus* species that suppress *daf-2*(*e1368*). A) Graphical representation of a novel platform for the identification of bacterial isolates that promote animal insulin signaling. Germ-free embryos were arrayed on a library of wild bacterial isolates and screened for development beyond the L4 stage. B) Percent of animals that developed past L4 on *Bacillus velezensis* NOBb103 and related species after 5 days at 26 °C. Experiments were performed in triplicate with ~500 animals per replicate. Error bars = s.d., **** = p < 0.0001 C) Representative images of *daf-2*(*e1368*) and *daf-1*(*m40*) on *E. coli* OP50, *B. subtilis* 168, and *P. lurida* MYb11. The animals were incubated at 26 °C for 5 days on their respective diets, washed in M9 buffer, and paralyzed with tetramisole. Scale bar is 1

mm. (D) Percent of *daf-2*(*e1368*) and (E) *daf-1*(*m40*) animals that developed past L4 on *E. coli* OP50, *B. subtilis* 168, and *P. lurida* MYb11 after 5 days at 26 °C. Experiments were performed in triplicate with ~500 animals per replicate. Error bars = s.d., **** = $p < 0.0001$, *** = $p < 0.0005$, ** = $p < 0.0023$

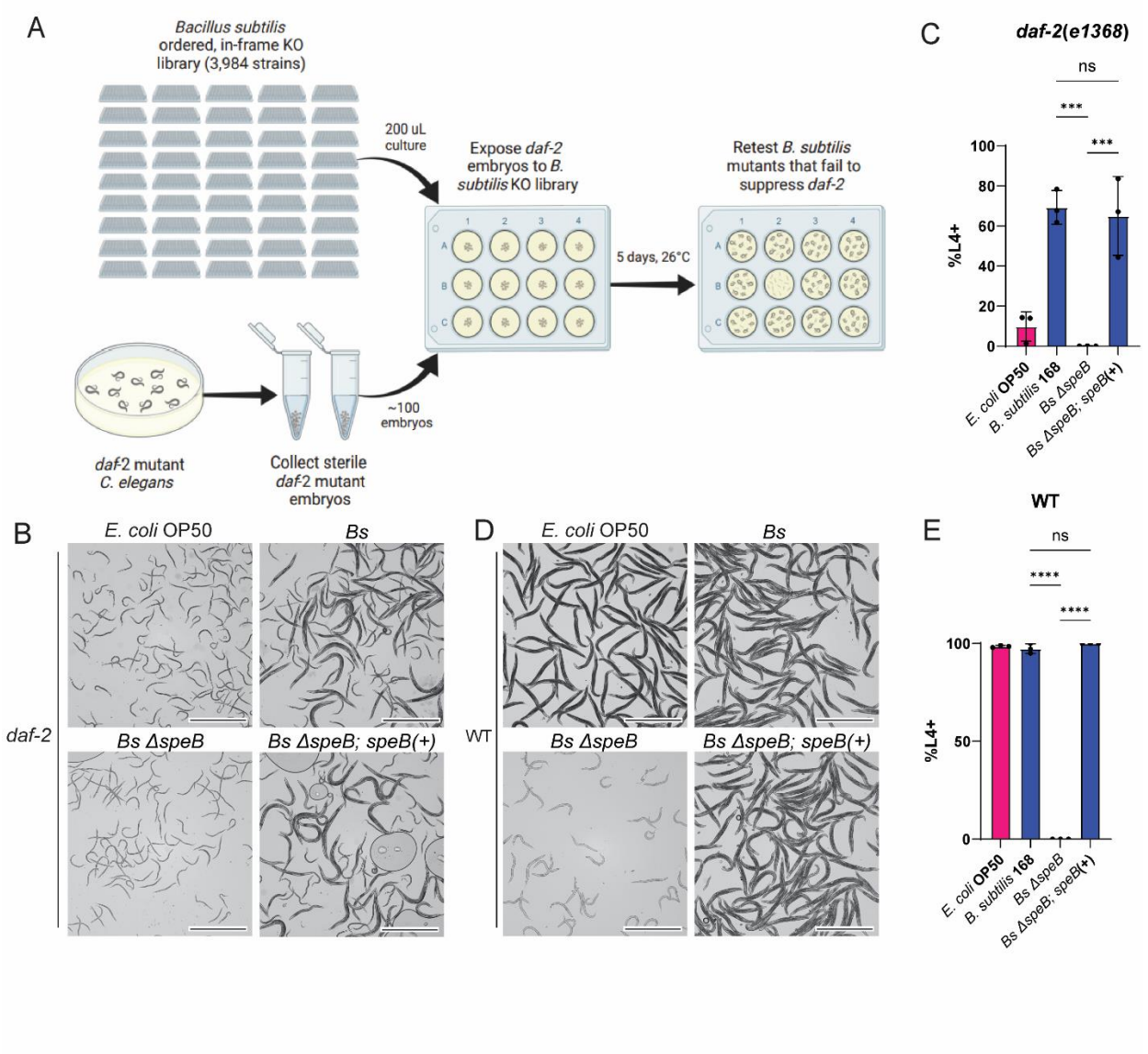

Figure 2: *B. subtilis speB* is required for *C. elegans* development. A) Graphical representation of the platform used to screen for mutants of *B. subtilis* that did not suppress *daf-2*(*e1368*). Germ-free embryos were arrayed on the library of 3,984 *B. subtilis* mutants and screened for development beyond the L4 stage after 5 days at 26 °C. Candidate mutants were retested on 60 mm plates with ~500 embryos. B) Representative images of *daf-2*(*e1368*) on *E. coli* OP50, *B. subtilis* 168 (*Bs*)(NOBb513), *Bs* Δ*speB* (NOBb514), and Bs Δ*speB; speB*(+) (NOBb475). The animals were incubated at 26 °C for 5 days on their respective diets, washed in M9 buffer, and

paralyzed with tetramisole. The scale bar is 1 mm. (C) Percentage of *daf-2*(*e1368*) fully developed animals on *E. coli* OP50, *B. subtilis* 168 (*Bs*)(NOBb513), *Bs* Δ*speB* (NOBb514), and *Bs* Δ*speB; speB*(+) (NOBb475) after 5 days at 26 °C. Error bars = s.d. *** = $p < 0.0002$, ns = not significant. (D) Representative images of WT on *E. coli* OP50, *B. subtilis* 168 (*Bs*)(NOBb513), *Bs* Δ*speB* (NOBb514), and Bs Δ*speB; speB*(+) (NOBb475). The animals were incubated at 26 °C for 5 days on their respective diets, washed in M9 buffer, and paralyzed with tetramisole. The scale bar is 1 mm. (E) Percentage of fully developed WT animals on *E. coli* OP50, *B. subtilis* 168 (*Bs*)(NOBb513), *Bs* Δ*speB* (NOBb514), and Bs Δ*speB; speB*(+) (NOBb475) after 5 days at 26 °C. Experiments were performed in triplicate with ~500 animals per replicate. Error bars = s.d. **** = $p < 0.0001$, ns = not significant

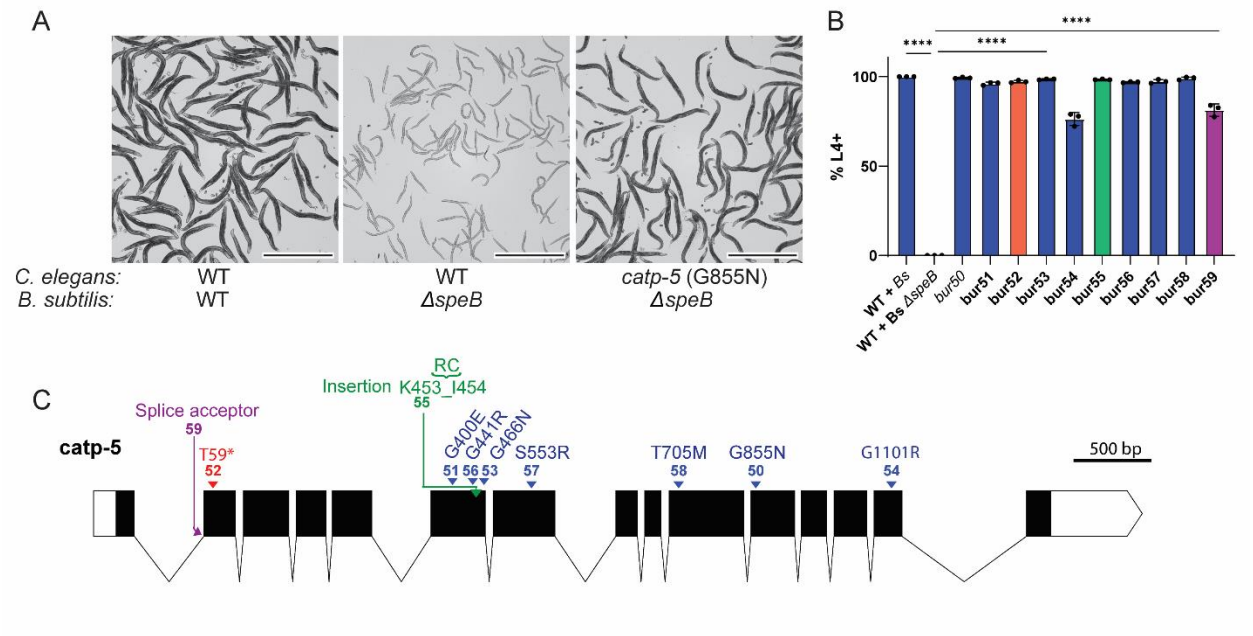

Figure 3: Mutations in the polyamine transporter, *catp-5*, confer resistance to *B. subtilis* Δ*speB*. (A) Representative images of WT *C. elegans* and mutant *catp-5*(*bur50*) on *B. subtilis* 168 (*Bs*)(NOBb513) and *B. subtilis* 168 Δ*speB* (NOBb514). The animals were incubated at 26 °C for 5 days on their respective diets, washed in M9 buffer, and paralyzed with tetramisole. The scale bar is 1 mm. (B) Percent of WT *C. elegans* (N2) and *catp-5*(*bur50-59*) that developed past L4 on *B. subtilis* 168 Δ*speB* (NOBb514) after 5 days at 26 °C. WT *C. elegans* on *B. subtilis* 168(*Bs*)(NOBb513) was included as a control. Experiments were performed in triplicate with ~500 animals per replicate. Error bars = s.d., **** = $p < 0.0001$ (C) Graphical representation of mutations in CATP-5 that restored animal development per allele (*bur50-59*). Red = nonsense mutation. Blue = nonsynonymous mutation. Green = insertion mutation. Purple = splice adaptor mutation. Numbers 50-59 correspond to allele *bur50-bur59*.

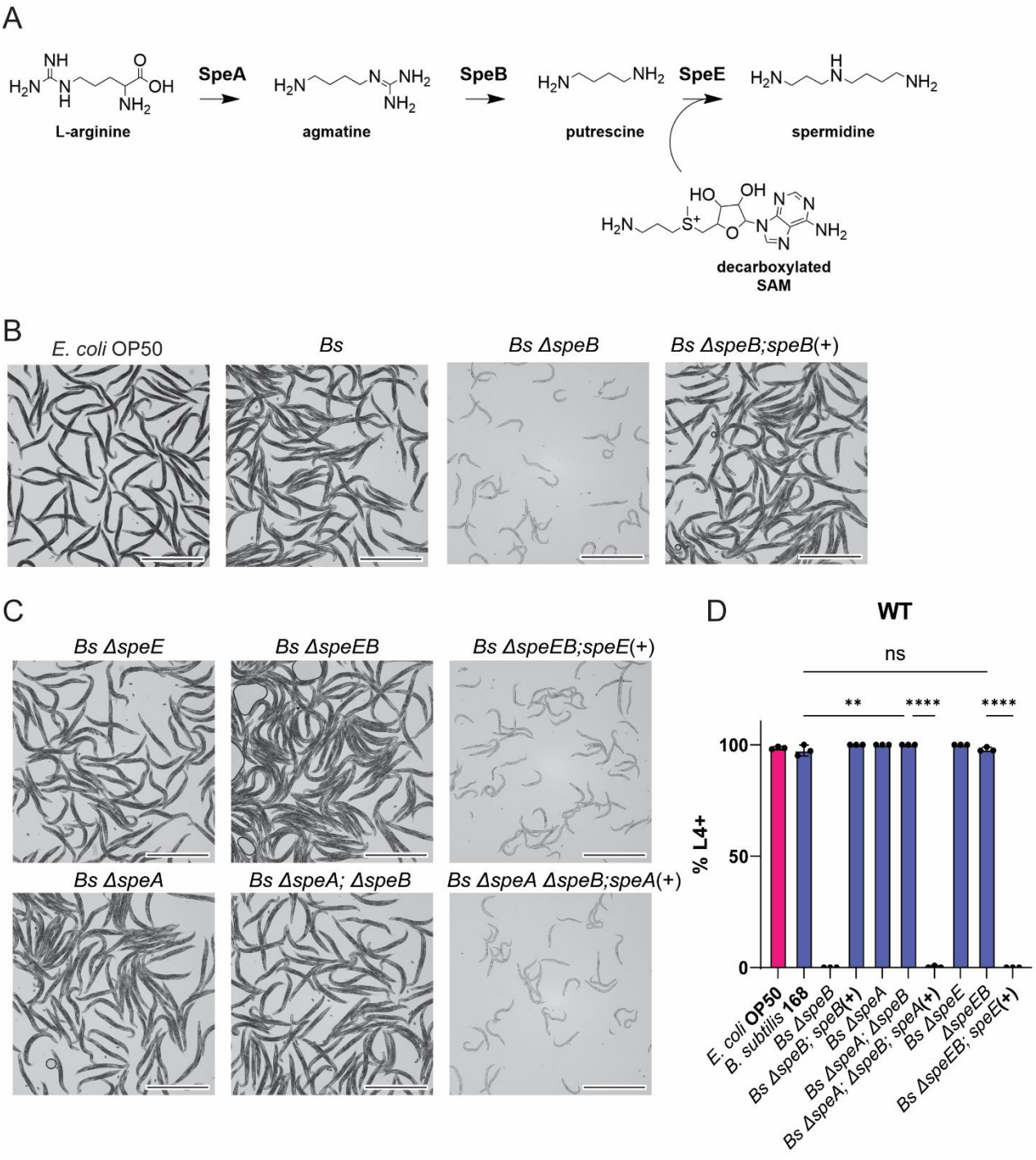

Figure 4: *speB* is the only gene in the canonical spermidine synthesis pathway that is required for *C. elegans* development. (A) Canonical spermidine synthesis pathway. (B) Representative images of WT *C. elegans* on *E. coli* OP50, *B. subtilis* 168 (NOBb513), *Bs* Δ*speB*

(NOBb514), and *Bs* Δ*speB; speB*(+) (NOBb475) (This figure is duplicated from Fig. 2D). Scale bars = 1 mm. (C) Representative images of WT *C. elegans* on *Bs* Δ*speE* (NOBb517), *Bs* Δ*speEB* (NOBb515), *Bs* Δ*speEB; speE* (+)(NOBb501), *Bs* Δ*speA* (NOBb516), *Bs* Δ*speB;* Δ*speA* (NOBb518), and *Bs* Δ*speA;* Δ*speB; speA*(+) (NOBb503).The animals were incubated at 26 °C for 5 days on their respective diets, washed in M9 buffer, and paralyzed with tetramisole. Scale bar is 1 mm. (D) Percent of WT *C. elegans* that developed past L4 when fed the strains reported in Fig. 4B and 4C after incubating for 5 days at 26 °C. Experiments were performed in triplicate with ~500 animals per replicate. Error bars = s.d., **** = $p < 0.0001$, ** = $p < 0.0065$, ns = not significant (The control strains data is the same data as Fig. 2E).

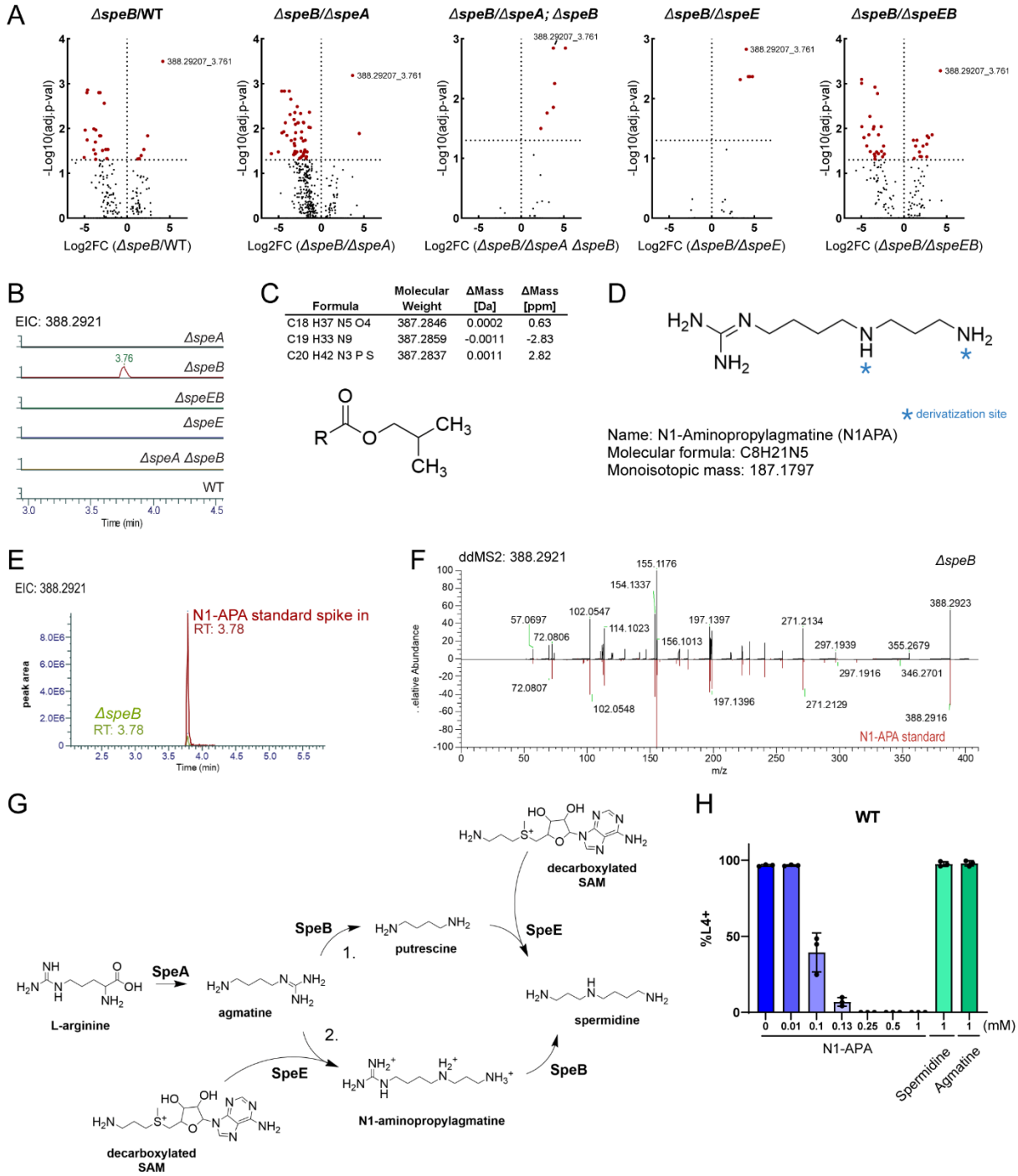

Figure 5. Identification and validation of N1-aminopropylagmatine (N1-APA) accumulated in *B. subtilis ΔspeB* cultures. (A) Volcano plots showing differential abundance analysis of untargeted metabolomics on carbamylated-derivatives in media between *ΔspeB* and other evaluated lines. Red dots are LC-MS features with an FDR adjusted P-value <0.05. Note the

feature 388.29207 m/z at retention time 3.781min is the most significantly elevated compound in each comparison. (B) Representative extracted ion chromatograms of 388.29207 m/z (+/- 5ppm). (C) Top, chemical formula predictions for m/z 388.29207 using accurate mass and fine isotopic structure in Compound Discoverer. Bottom, structure of carbamylated-derivatives indicate two oxygens are present in each derivatized moiety. (D) Structure of N1-aminopropylagmatine with sites of carbamylated-derivatives denoted with a blue asterisk. Note the chemical formula of N1-aminopropylagmatine ($C_8H_{21}N_5$) with carbamylated-derivatives ($C_5H_9O_2$ x2) at the indicated sites match the predicted chemical formula of the unknown ($C_{18}H_{37}N_5O_4$). (E) Overlaid extracted ion chromatograms of *ΔspeB* and *ΔspeB*+N1APA spike-in provides accurate mass and chromatographic profile confirmation of N1APA as the unknown feature 388.29207@3.7981min. (F) Data dependent MS2 fragmentation mirror plot of parent ion 388.29207@3.7981min in *ΔspeB* (top) and neat N1-APA standard (bottom) provides further confirmation that the unknown is N1-APA. (G) Canonical spermidine synthesis pathway (1.) compared to the alternative pathway (2.) found in *Thermus thermophilus*, which includes N1-aminopropylagmatine as an intermediate metabolite. (H) Percent of WT *C. elegans* (N2) that developed past L4 when grown on media supplemented with a range of concentrations of N1-APA and seeded with wild type *B. subtilis* after incubating for 3 days at 20 °C. Control plates were supplemented with 1 mM agmatine and spermidine. Experiments were performed in triplicate with ~200 animals per replicate. Error bars = s.d. **** = $p < 0.0001$

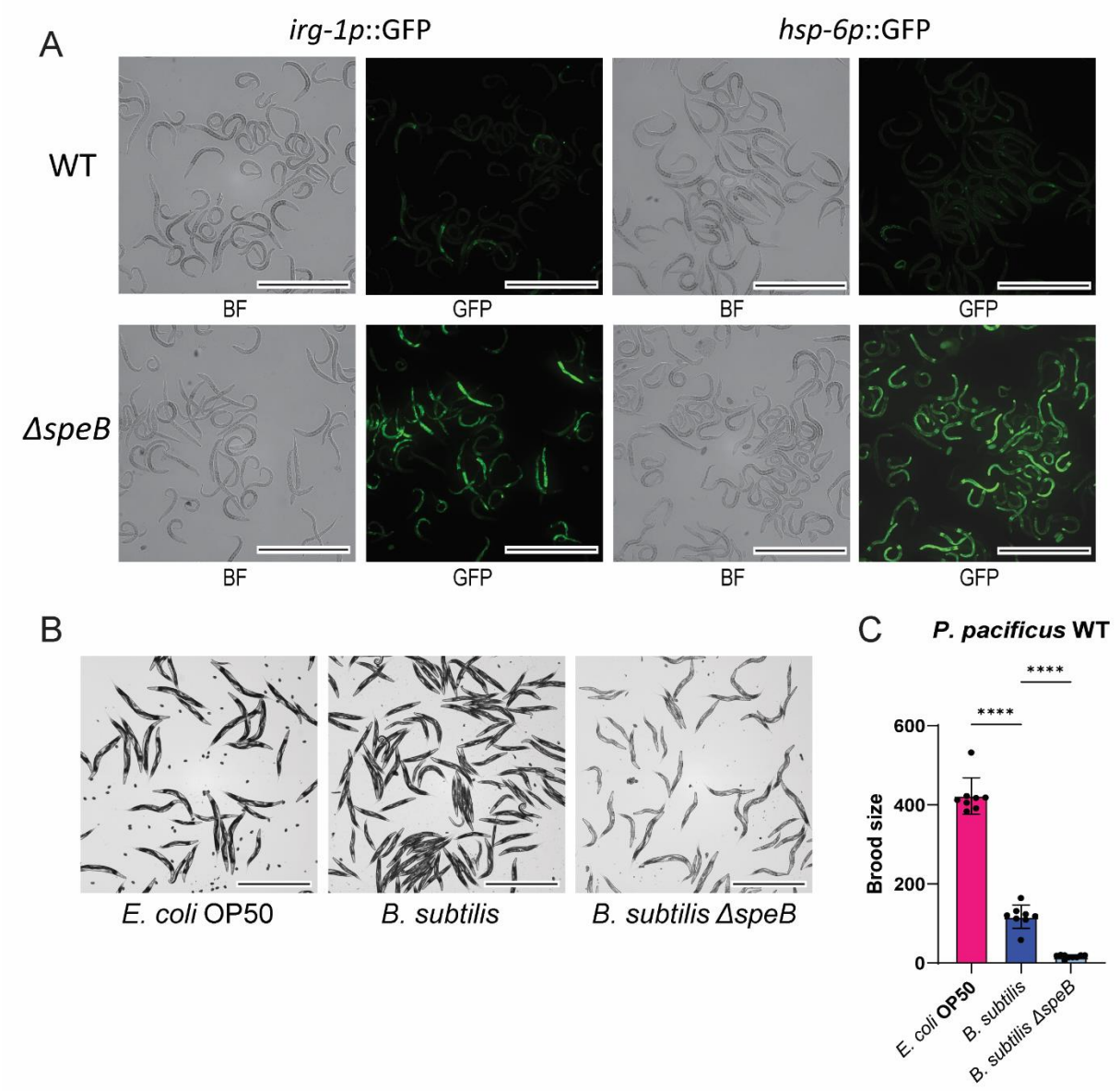

Figure 6: N1-aminopropylagmatine-induced developmental arrest is mediated by mitochondrial stress. (A) Brightfield (BF) and fluorescent (GFP) images of growth stage matched *irg-1p::GFP* and *hsp-6p::GFP* on a diet of *B. subtilis* (NOBb513) or *B. subtilis* Δ*speB* (NOBb514). The *C. elegans* strains were incubated on the respective *B. subtilis* strains for ~30 hours at 20 °C. Representative images were pseudo-colored using ImageJ v1.54f. Scale bars are 0.5 mm. (B) Representative images of *Pristionchus pacificus* on a diet of *E. coli* OP50, *B. subtilis*, and *B. subtilis* Δ*speB* (NOBb369). Scale bars are 1 mm. (C) Quantification of brood size

in *P. pacificus* on a diet of *E. coli* OP50, *B. subtilis*, and *B. subtilis* Δ*speB* (NOBb369). Error bars = s.d., **** = $p < 0.0001$

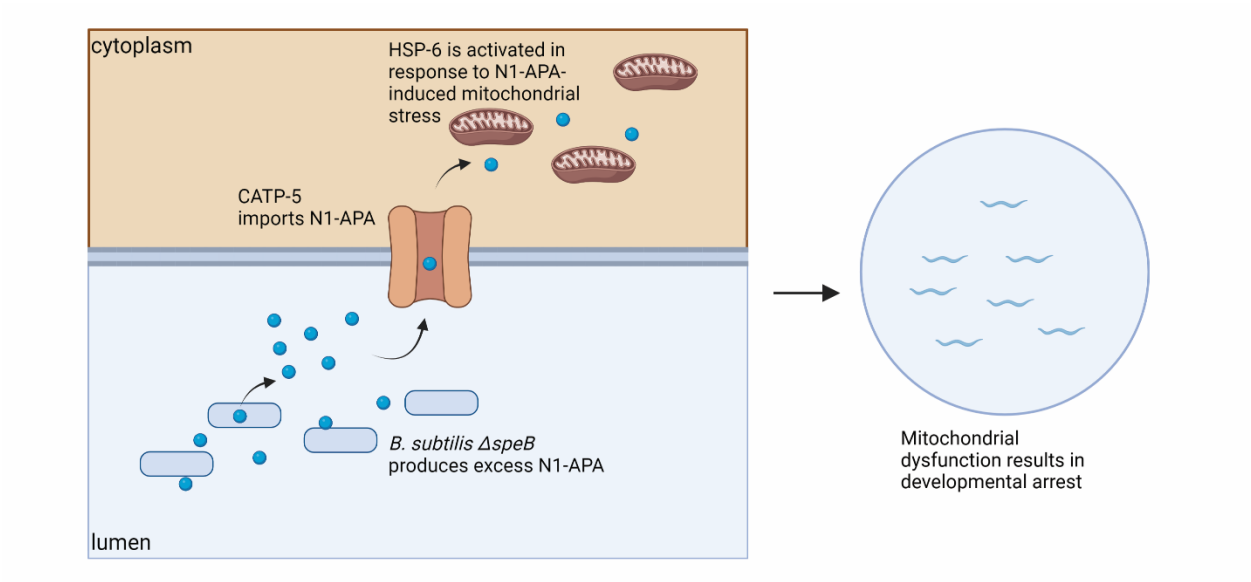

Figure 7: Model for N1-aminopropylagmatine-mediated loss of *C. elegans* development. N1-animopropylagmatine accumulates in the C. elegans intestinal lumen when the animals are grown on a diet of *B. subtilis* Δ*speB*. CATP-5 transports N1-aminopropylagmatine into intestinal cells where it antagonizes normal mitochondrial function. N1-aminopropylagmatine likely antagonizes mitochondrial function which results in developmental arrest before the animals reach the L4 developmental stage.

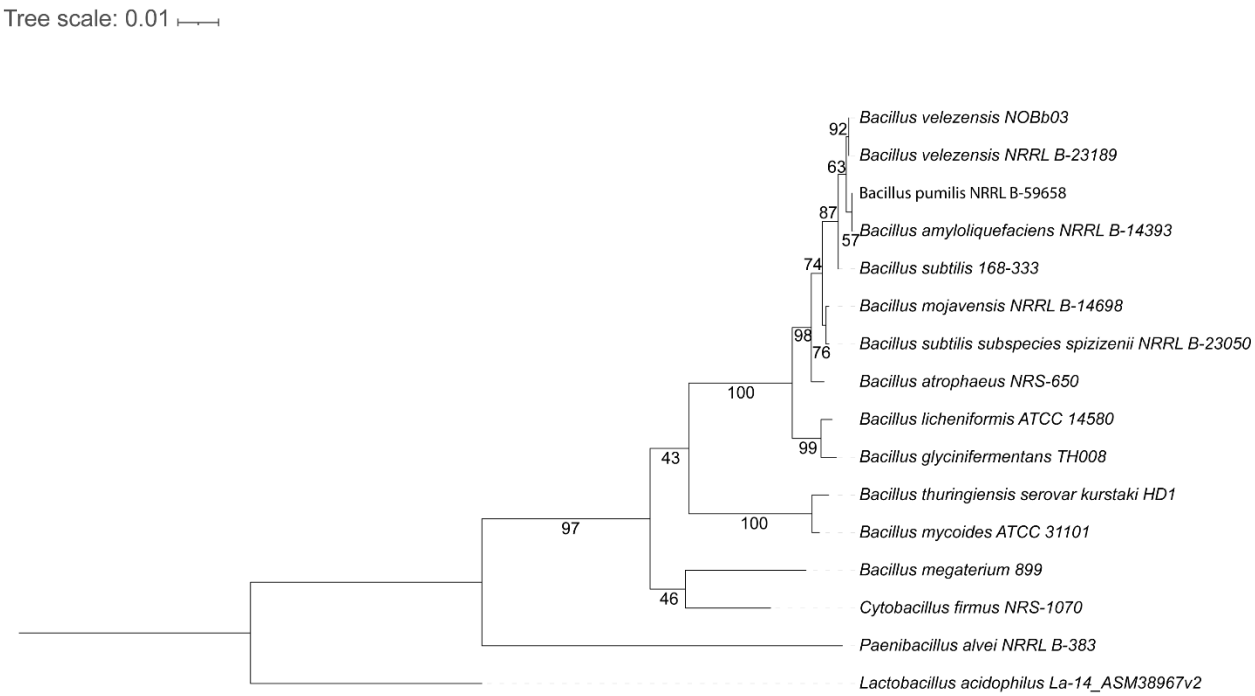

Supplementary Figure 1: Maximum-likelihood-based phylogenetic tree of *Bacillus* species tested in Fig. 1B. 16S rRNA sequencing was performed at Genewiz. *Lactobacillus acid ophilus* La-14 (ASM38967v2) was used as a root.

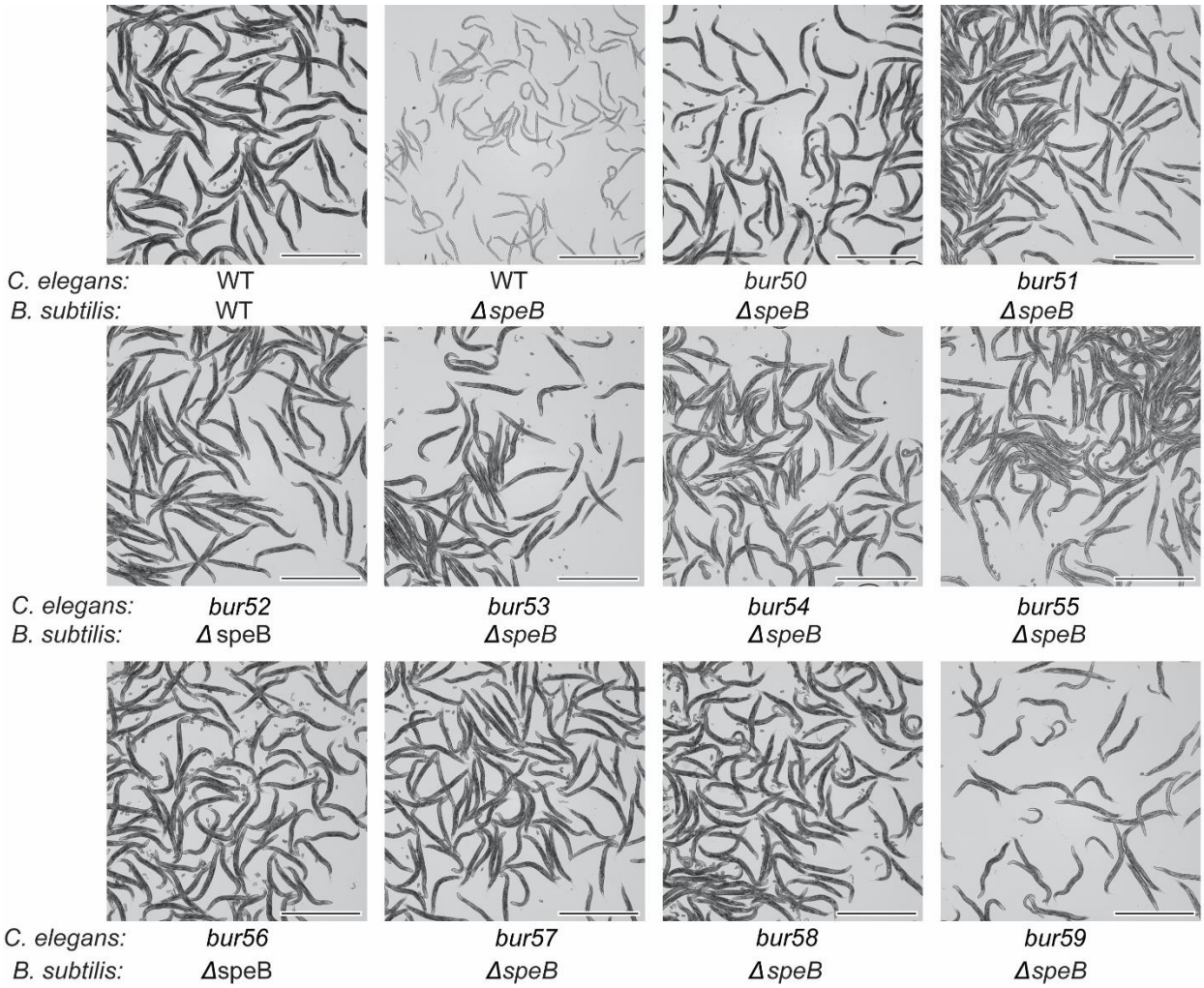

Supplementary Figure 2: mutations in *catp-5* promote *C. elegans* development on a diet of *B. subtilis* Δ*speB*. Representative images of WT and *catp-5* (*bur50-59*) on a diet of *B. subtilis* Δ*speB* (NOBb369) after incubation at 20 °C for 3 days. Scale bars = 1 mm.

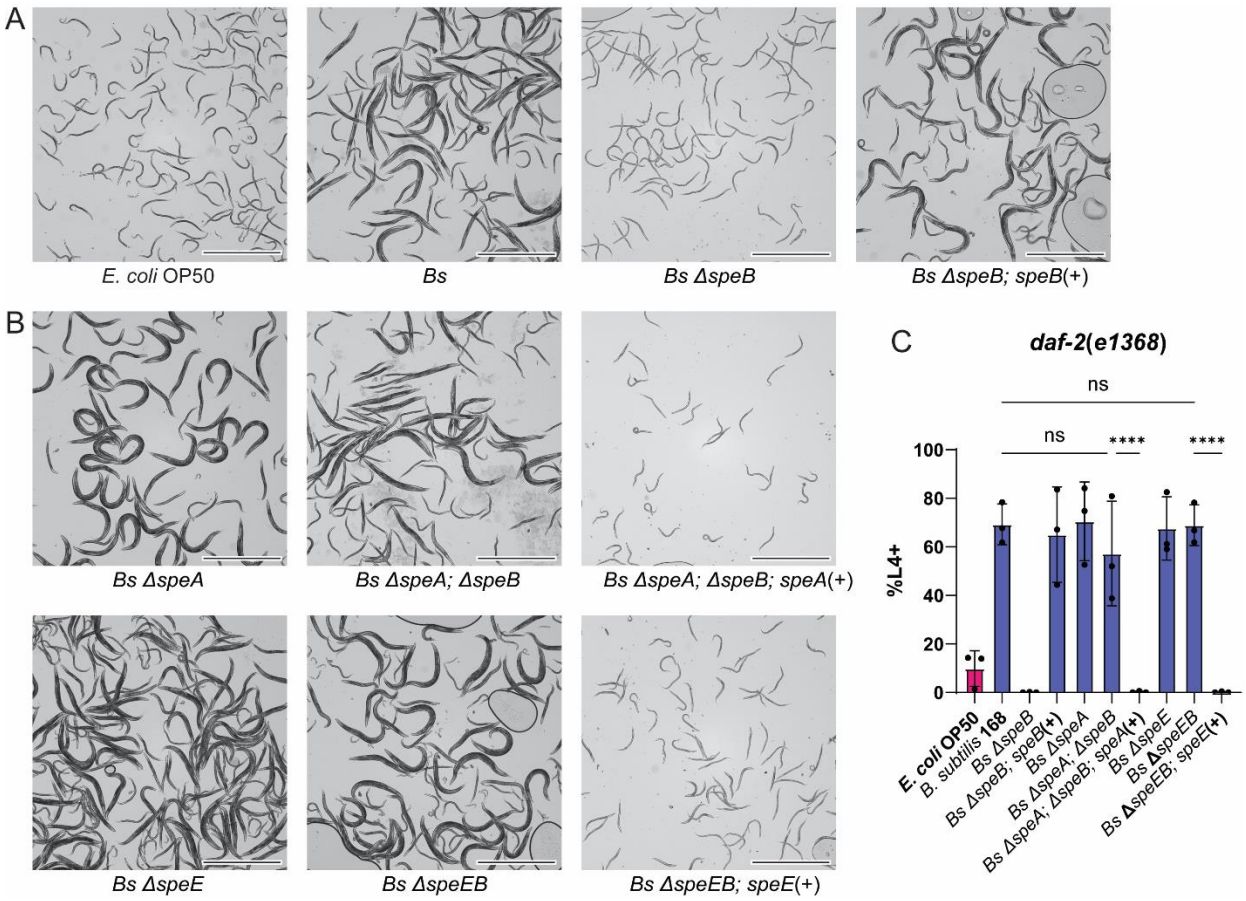

Supplementary Figure 3: *B. subtilis speB* is required for *daf-2(e1368)* development. (A) Representative images of *daf-2*(*e1368*) on *E. coli* OP50, *B. subtilis* (*Bs*) (NOBb513), *Bs* Δ*speB* (NOBb514), *Bs* Δ*speB; speB*(+) (NOBb475), (B) *Bs* Δ*speE* (NOBb517), *Bs* Δ*speEB* (NOBb515), *Bs* Δ*speEB; speE*(+) (NOBb501), *Bs* Δ*speA* (NOBb516), *Bs* Δ*speA;* Δ*speB* (NOBb518), and *Bs* Δ*speA;* Δ*speB; speA*(+) (NOBb503).The animals were incubated at 26 °C for 5 days on their respective diets, washed in M9 buffer, and paralyzed with tetramisole. Scale bars = 1 mm. (C) Percent of *daf-2*(*e1368*) that developed past L4 when fed the *Bacillus subtilis* strains reported in SFig. 2A after incubating for 5 days at 26 °C. Experiments were performed in triplicate with ~500 animals per replicate. Error bars = s.d., **** = $p < 0.0001$, ns = not significant (The data for the control strains is duplicated from Fig. 2B and C).

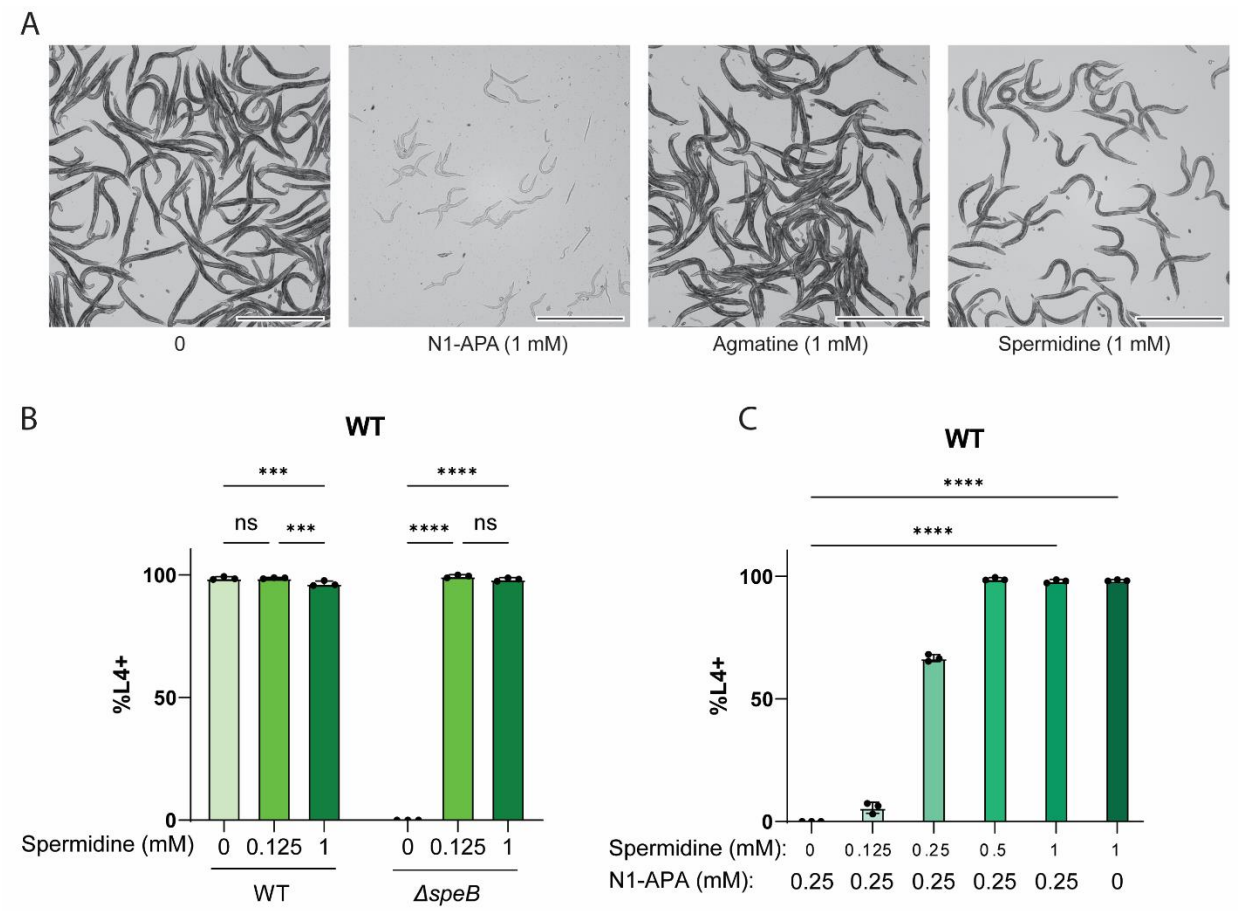

Supplementary Figure 4: Exogenous spermidine suppresses the effects of N1-aminopropylagmatine on animal development. (A) Representative images from Fig. 5H of WT *C. elegans* grown on modified NGM (see methods) seeded with *B. subtilis* WT (0) and supplemented with N1-aminopropylagmatine (N1-APA) (1 mM), agmatine (1 mM), or spermidine (1 mM). Scale bar = 1 mm. (B) Percent of WT *C. elegans* that develop past L4 on modified NGM (see methods) supplemented with 0.25 mM N1-aminopropylagmatine and a concentration gradient of spermidine (0.125 - 1 mM). Error bars = s.d. **** = $p < 0.0001$. (C) Percent of WT *C. elegans* that developed past L4 on modified NGM (see methods) seeded with *B. subtilis* (WT) or *B. subtilis* Δ*speB* (NOBb369) and supplemented with spermidine (0.125 and 1 mM). Error bars = s.d., *** = $p < 0.008$, **** = $p < 0.0001$, ns = not significant.

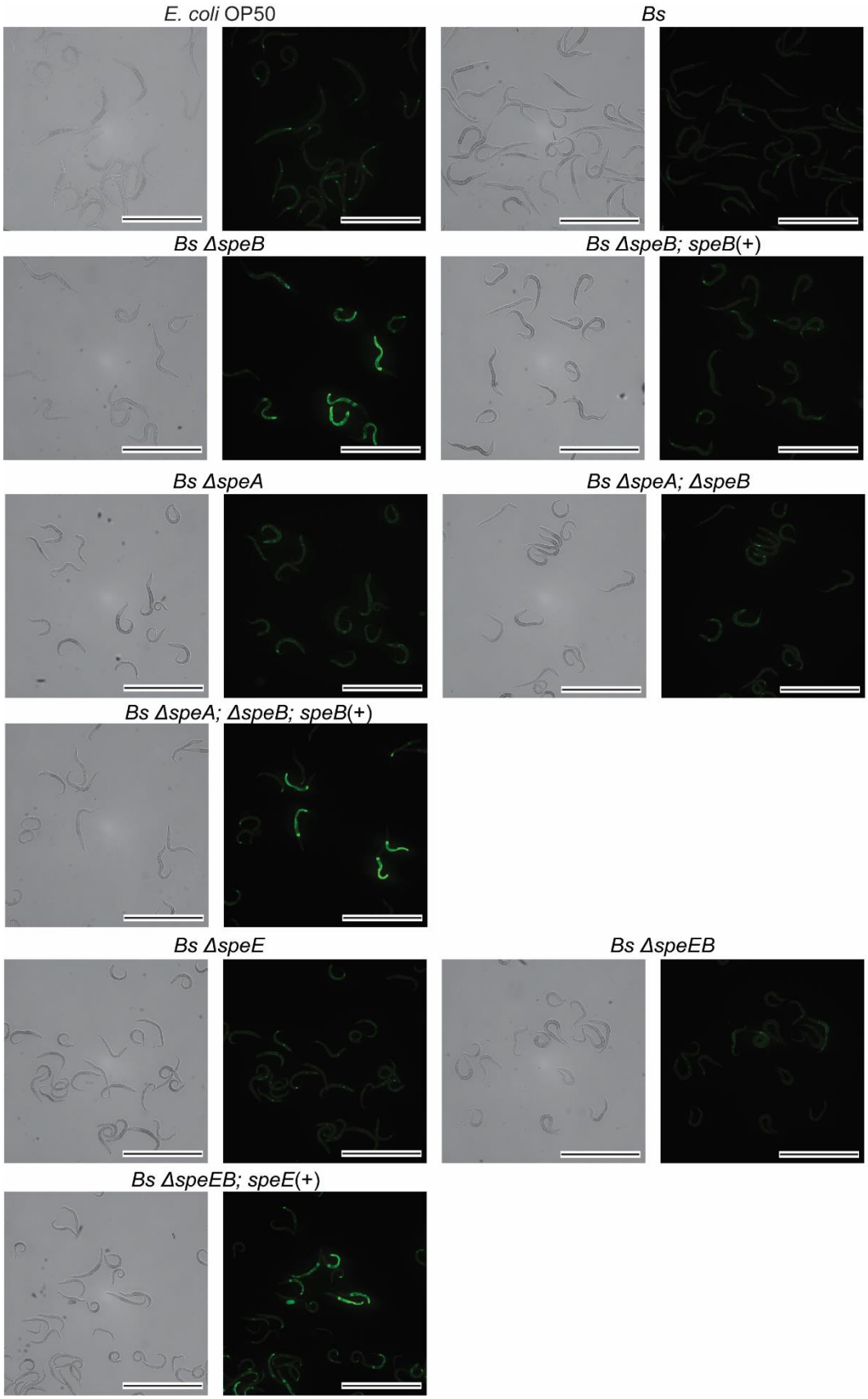
E. coli OP50
Bs
Bs ΔspeB
Bs ΔspeB; speB(+)
Bs ΔspeA
Bs ΔspeA; ΔspeB
Bs ΔspeA; ΔspeB; speB(+)
Bs ΔspeE
Bs ΔspeEB
Bs ΔspeEB; speE(+)

Supplementary Figure 5: N1-aminopropylagmatine-induced developmental arrest is mediated by mitochondrial stress. A) Brightfield (BF) and fluorescent (GFP) images of growth stage matched *hsp-6p::GFP*, on *E. coli* OP50, *B. subtilis* (NOBb513), *Bs* Δ*speB* (NOBb514), *Bs* Δ*speB; speB*(+) (NOBb475), (B) *Bs* Δ*speE* (NOBb517), *Bs* Δ*speEB* (NOBb515), *Bs* Δ*speEB; speE*(+) (NOBb501), *Bs* Δ*speA* (NOBb516), *Bs* Δ*speA;* Δ*speB* (NOBb518), and *Bs* Δ*speA;* Δ*speB; speA*(+) (NOBb503). The *C. elegans* strains were incubated on the respective *B. subtilis* strains for ~30 hours at 20 °C. Representative images were pseudo-colored using ImageJ v1.54f. Scale bars = 0.5 mm.

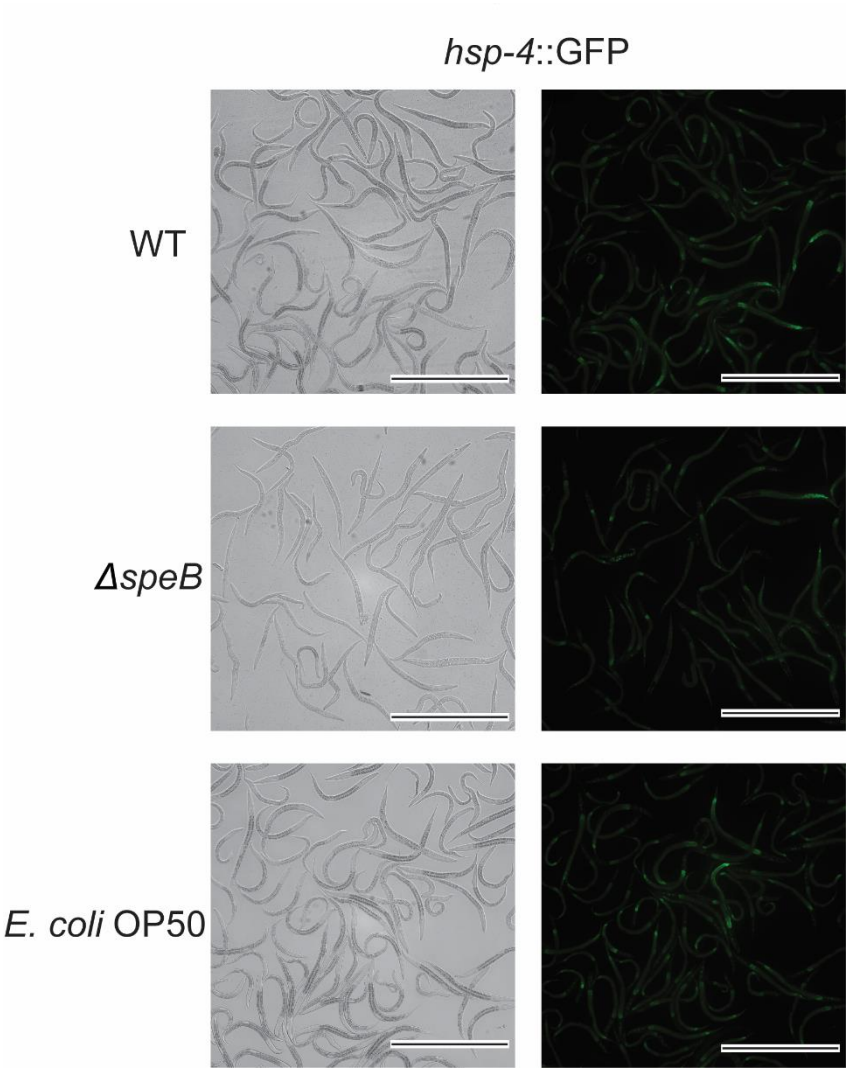

Supplementary Figure 6: *hsp-4* is not activated by N1-aminopropylagmatine. Brightfield (BF) and fluorescent (GFP) images of growth stage matched *hsp-4p::GFP*, on *E. coli* OP50, *B. subtilis* (WT), and *Bs* Δ*speB* (NOBb369). Representative images were pseudo-colored using ImageJ v1.54f. Scale bars = 0.5 mm.

	Position	Refer-ence	Alter-nate	Variant Type	CDS Variant Annotation	Protein Variant Annota-tion	Alternate Allele Depth
bur50	8092275	C	T	missense_variant	c.4267G>A	p.Gly855Asp	103
bur51	8094229	C	T	missense_variant	c.2313G>A	p.Gly400Glu	95
bur52	8095771	C	T	stop_gained	c.770G>A	p.Trp59*	106
bur53	8094031	C	T	missense_variant	c.2510G>A	p.Gly466Asp	112
bur54	8091401	C	T	missense_variant	c.5141G>A	p.Gly1101Arg	65
bur55	8095831	C	T	splice_acceptor_variant	c.118-1G>A	intron	78
bur56	8094107	C	T	missense_variant	c.2435G>A	p.Gly441Arg	103
bur57	8093719	A	T	missense_variant	c.2822T>A	p.Ser553Arg	93
bur58	8092772	G	A	missense_variant	c.3770C>T	p.Thr705Met	98
bur59	8094738	G	A	insertion	c.1059+11C>T	p.Lys453-Iso454 in-sArgCys	73

Table 1: List of mutations in *catp-5* that result in *C. elegans* development on *B. subtilis* Δ*speB*

	nlp-29p	*clec-60p*	*gcs-1p*	*hsp-60*	*hsp-16.2p*	*gst-4p*	*hsp-4*	*irg-1p*	*sod-3p*	*bvIs5*	*hsp-6p*
Difference between WT and *ΔspeB*	-	-	-	-	-	-	-	+	-	-	+

Table 2: Summary of *C. elegans* GFP reporter strains on a diet of *B. subtilis 168* Δ*speB*.

Strain	**Description**	**Reference**
P. pacificus		
PS312	*P. pristioncus* wild isolate	(38)
C. elegans		
N2	*Caenorhabditis elegans* wild isolate	(38)
DR1572	*C. elegans daf-2(e1368) III*	(38)
DR40	*C. elegans daf-1(m40) IV*	(38)
NOB159	*catp-5(bur50) G855N*	this study
NOB160	*catp-5(bur51) G400E*	this study
NOB161	*catp-5(bur52) W59**	this study
NOB162	*catp-5(bur53) G466N*	this study
NOB163	*catp-5(bur54) G1101R*	this study
NOB164	*catp-5(bur55) intron variant*	this study
NOB165	*catp-5(bur56) G441R*	this study
NOB166	*catp-5(bur57) S553R*	this study
NOB167	*catp-5(bur58) T705M*	this study
NOB168	*catp-5(bur59) intron variant*	this study
IG274	*frIs7 [nlp-29p::GFP + col-12p::DsRed] IV*	(38)
JIN810	*agIs26 [clec-60p::GFP + myo-2p::mCherry]*	(38)
LD1171	*ldIs3 [gcs-1p::GFP + rol-6(su1006)]*	(38)
SJ4058	*zcIs9 [hsp-60::GFP + lin-15(+)]*	(38)
WE5172	*ajIs1 [rCesC05A9.1::GFP + dpy-5(+)] X*	(38)
CL2070	*dvIs70 [hsp-16.2p::GFP + rol-6(su1006)]*	(38)
CL2166	*dvIs19 [(pAF15)gst-4p::GFP::NLS] III*	(38)
SJ4005	*zcIs4 [hsp-4::GFP] V*	(38)
AU133	*agIs17 [myo-2p::mCherry + irg-1p::GFP] IV*	(38)
CF1553	*muIs84 [(pAD76) sod-3p::GFP + rol-6(su1006)]*	(38)
CY573	*bvIs5 [cyp-35B1p::GFP + gcy-7p::GFP]*	(38)
GL347	*zcIs13 [hsp-6p::GFP + lin-15(+)] V*	(38)
B. subtilis		

BGSCID: 1A1	*B. subtilis 168 trpC2*	(39)
NOBb369	*B. subtilis 168 ΔspeB*	this study
NOBb475	*B. subtilis 168 ΔspeB thrC::P_{speEB}-speB (pNOB47)*	this study
NOBb501	*B. subtilis 168 ΔspeEB thrC::P_{speEB}-speE (pNOB48)*	this study
NOBb503	*B. subtilis 168 ΔspeB speA::kanR thrC::P_{speA}-speA (pNOB49)*	this study
NOBb513	*B. subtilis 168 thrC::pDG1664*	this study
NOBb514	*B. subtilis 168 ΔspeB thrC::pDG1664*	this study
NOBb515	*B. subtilis 168 ΔspeEB thrC::pDG1664*	this study
NOBb516	*B. subtilis 168 speA::kanR thrC::pDG1664*	this study
NOBb517	*B. subtilis 168 speE::kanR thrC::pDG1664*	this study
NOBb518	*B. subtilis 168 ΔspeB speA::kanR thrC::pDG1664*	this study
E. coli		
OP50	*ura-, strR, rnc-, (delta)attB::FRT-lacI-lacUV5p-T7)*	
Bacillus species		
NRRL B-23189	*Bacillus velezensis* NRRL B-23189	NRRL USDA strain collection
NRRL B-59658	*Bacillus pumilis* NRRL B-59658	NRRL USDA strain collection
NRRL B-14698	*Bacillus mojavensis* NRRL B-14698	NRRL USDA strain collection
NRRL B-14393	*Bacillus amyloliquefaciens* NRRL B-14393	NRRL USDA strain collection
NRRL B-23050	*Bacillus subtilis subspecies spizizenii* NRRL B-23050	NRRL USDA strain collection
NOBb267	*Bacillus velezensis*	this study
HD1	*Bacillus thuringiensis serovar kurstaki* HD1	BGSC
ATCC 14580	*Bacillus licheniformis* ATCC 14580	BGSC
TH008	*Bacillus glycinifermentans* TH008	BGSC
ATCC 31101	*Bacillus mycoides* ATCC 31101	NRRL USDA strain collection
899	*Bacillus megaterium* 899	NRRL USDA strain collection

NRS-650	*Bacillus atrophaeus* NRS-650	NRRL USDA strain collection
NRS-1070	*Cytobacillus firmus* NRS-1070	NRRL USDA strain collection
NRRL B-383	*Paenibacillus alvei* NRRL B-383	NRRL USDA strain collection

Table 3: List of nematode and bacterial strains used in this study.

Plasmid	Relevant features	Parent vector	Restriction enzymes to digest parent vector	PCR primers	PCR template	Reference
pDG1664	*thrC, amp, erm, spec*	N/A	N/A	N/A	N/A	(54)
pMAD	*amp, erm, ori-pE194ts*	N/A	N/A	N/A	N/A	(55)
pNOB41	pMAD Δ*speEB*	pMAD	BglII, EcoRI	KN429-KN432	*B. subtilis* 168	this study
pNOB47	*thrC::P_{speEB}-speB amp erm spec*	pDG1664	BamHI, EcoRI	KN475-KN478	*B. subtilis* 168	this study
pNOB48	*thrC::P_{speEB}-speE amp erm spec*	pDG1664	BamHI, EcoRI	KN492, KN493	*B. subtilis* 168	this study
pNOB49	*thrC::P_{speA}-speA amp erm spec*	pDG1664	BamHI, EcoRI	KN490, KN491	*B. subtilis* 168	this study

Table 4: List of plasmids used in this study

Oligo name	Sequence	Relevant features
KN429	ACACATTAACTAGACAGATCACCGTTGTATAGAC-GTTTAA	Clone ~1 kb upstream *speEB* into pMAD digested with BglII and EcoRI FOR
KN430	GACATCGTCTGGATGTTTACTAAAAAC-GATCTTTTTTTCTCATAATAGT	Clone ~1 kb upstream speEB into pMAD digested with BglII and EcoRI REV
KN431	ACTATTATGAGAAAAAAAGATCGTTTTTAG-TAAACATCCAGACGATGTC	Clone ~1 kb downstream *speEB* into pMAD digested with BglII and EcoRI FOR
KN432	CTGCAGAAGCTTCTAGAATTCGGA-GATGTAATATATTTATCAGAGT	Clone ~1 kb downstream speEB into pMAD digested with BglII and EcoRI REV
KN475	AAAACTGCTGCCTTCGGATCAACATCG-CAGAACAGGACGC	Clone 144 bp P_{speEB} promoter into pDG1664 digested with BamHI and EcoRI FOR
KN476	TAAGCTTCATCAAATCTcatTT-GTCATCTCCCTTTCGAGG	Clone 144 bp P_{speEB} promoter into pDG1664 digested with BamHI and EcoRI REV
KN477	CCTCGAAAGGGAGATGACAAatgAGATTTGATGAA-GCTTATTCA	Clone *speB* into pDG1664 digested with BamHI and EcoRI FOR
KN478	AACTTTAGGGTTATCGAATTttaTTTCACAAACCCAA-GCAG	Clone *speB* into pDG1664 digested with BamHI and EcoRI REV
KN490	AAAACTGCTGCCTTCGGATCTTTCTTCACTCCTT-GTAGATTTAC	Clone speA with 184 bp P_{speA} promoter into pDG1664 digested with BamHI and EcoRI FOR
KN491	AACTTTAGGGTTATCGAATTttaTTGAATTGCTTTTT-GTTCTTTG	Clone speA with 184 bp P_{speA} promoter into pDG1664 digested with BamHI and EcoRI REV
KN492	AAAACTGCTGCCTTCGGATCAAC-GGGTTCCCCCTTTTTTT	Clone speE with 201 bp P_{speEB} promoter into pDG1664 digested with BamHI and EcoRI FOR

KN493	AACTTTAGGGTTATCGAATTTTATTTAATCAGGTCAC TCACAAA	Clone speE with 201 bp P_{speEB} promoter into pDG1664 digested with BamHI and EcoRI REV

Table 5: List of oligonucleotides used in this study

DATA AVAILABILITY

All data reported in this paper are available in the Statistics Source Data.

QUANTIFICATION AND STATISTICAL ANALYSIS

One way ANOVA p-value calculations were performed in GraphPad Prism 10.1.2 (324) (40) and were used to determine statistical significance for figures: 1B, 1D, 1E, 2D, 2E, 3B, 4D, 5H, 6C, SFIG 3C, SFIG 4B, and SFIG 4C.

METHOD DETAILS

C. elegans growth media and conditions

C. elegans strains were maintained at 15 °C or 20 °C on NGM agar plates (3 g/L NaCl, 17 g/L Agar, 2.5 g/L peptone (Bacto), 25 mM KPO_4 (pH 6), 5 mg/L Cholesterol, 1 mM $MgSO_4$, 1 mM $CaCl_2$) seeded with *E. coli* OP50 (CGC, DA837). All *C. elegans* strains used in this study are listed in Table 3. *C. elegans* that were fed a diet of *B. subtilis* or *B. subtilis* mutants for experimentation were grown on modified NGM (3 g/L NaCl, 17 g/L Agar, 5.0 g/L peptone (Bacto), 25 mM KPO_4 (pH 9.2), 5 mg/L Cholesterol, 1 mM $MgSO_4$, 1 mM $CaCl_2$).

Egg Prep Protocol

Adult *C. elegans* were washed from NGM agar plates with M9 buffer (3 g/L KH_2PO_4, 6 g/L Na_2HPO_4, 5 g/L NaCl, 1 mM $MgSO_4$). *C. elegans* were lysed with Egg Preparation Solution (30% Sodium hypochlorite, 1 M NaOH) and monitored by dissection microscope for ~1-3 minutes. The embryos were washed 2-3 times in M9 buffer.

Bacteria growth media and conditions

All bacterial strains were grown on Lennox LB Agar (5 g/L NaCl, 10 g/L SELECT Peptone 140, 5 g/L SELECT Yeast Extract) (Invitrogen, 12780029) at 30 °C or 37 °C unless specified otherwise

and are listed in Table 3. Liquid cultures were grown at 30 °C and shaken in <5 mL Lennox LB at 220 rpm in 18 mm glass test tubes. *Bacillus* strains containing pDG1664 and its derivatives inserted at *thrC* were grown in Lennox LB containing MLS (25 µg/mL erythromycin (Thermo Fisher Scientific, 50-213-296) and 5 µg/mL lincomycin (Thermo Fisher Scientific, 50-213-395)). Bacillus non-essential gene knock out library mutants were grown in kanamycin (7.5 µg/mL (Sigma, K1377)). Plasmid selection in *E. coli* was performed on Lennox LB containing kanamycin (25 µg/mL, Sigma Aldrich, K1377) or ampicillin (100 µg/mL, Sigma Aldrich, A0166).

Bacteria strains and plasmid construction

All plasmids were constructed by isothermal assembly (ITA) and are listed in Table 4. DNA regions for plasmid assembly were identified using Biocyc (41) and amplified by touchdown PCR from the bacterial chromosomes using Q5 DNA polymerase (New England Biolabs, M0492) and oligonucleotides from Integrated DNA Technologies (Coralville, IA) listed in Table 5. All oligonucleotides are listed in Table 5. PCR fragments were purified using the Monarch DNA Gel Extraction Kit (New England Biolabs, T1020) and assemblies were performed using the NEBuilder HiFi DNA Assembly Master Mix (New England Biolabs, E2621). All regions amplified by PCR were confirmed by DNA sequencing at Genewiz from Azenta Life Sciences (South Plainfield, NJ). Plasmids were transformed according to the manufacturer's instructions and maintained in *E. coli* DH5α competent cells (New England Biolabs, C2988J). Plasmids or purified chromosomal DNA were transformed into *B. subtilis* strains by natural competency as previously described (17).

All *Bacillus subtilis* strains reported in this study are isogenic derivatives of *B. subtilis* 168 (BGSCID: 1A1) and are reported in Table 3. The operon encoding *speEB* was knocked out by homologous recombination using the suicide vector, pMAD (42). Approximately 1 kb upstream and downstream of *speEB* were amplified and assembled via ITA into pMAD digested with BglII and EcoRI (New England Biolabs, R0144 and R3101, respectively), resulting in plasmid

pNOBb41 (Table 4). The deletion was confirmed by PCR, sanger sequencing, and whole genome sequencing.

Strain NOBb518 was constructed by transforming purified chromosomal DNA (see methods section: *Bacillus* genomic DNA extraction) from strain BKK14630 (*speA::kanR*) (17) into NOBb369 (Δ*speB*). Chromosomal DNA was transformed by natural competency as previously described (17).

Plasmids for complementation studies (pNOB47, pNOB48, and pNOB49) were constructed by amplifying target genes from the *Bacillus subtilis* 168 chromosome using the primers listed in Table 4. These amplicons were assembled in pDG1664 digested with EcoRI and HindIII (New England Biolabs, R3101 and R3104, respectively) by ITA and were expressed under the control of their respective native promoters. When necessary *kanR* was removed from the *Bacillus subtilis* chromosome using pDR244 (17) (Bacillus Genetic Stock Center, BGSCID ECE274).

Screen of wild bacterial isolates for *C. elegans* development

Compost samples from the Grand Rapids, MI area were collected, diluted in M9 buffer, filtered, and plated on LB. Single colonies were grown overnight at 30 °C and 200 µL of culture was seeded on NGMB 12-well plates. The plates were dried in a laminar flow hood. Approximately 100-200 germ-free *C. elegans daf-2* (DR1572) embryos were added to each well. The plates were incubated for 5 days at 26 °C. The abundance of L4+ animals was qualified by eye using a dissection microscope. Strains of bacteria that promoted *C. elegans* development were retested on 90 mm NGM plates to confirm.

Screen of *B. subtilis* 168 knockout library for loss of *C. elegans* development

The *B. subtilis* single gene deletion library--kanamycin was acquired from Addgene (Watertown, MA, 1000000115). The parent strain was acquired from the Bacillus Genetic Stock Center (Columbus, OH, BGSCID: 1A1). The library was replicated into 96-well plates for further use.

Each 96-well plate was replicated and incubated overnight at 30 °C in LB. Each well was seeded on NGMB in a 12-well plate and dried in a laminar flow hood. 50-100 *C. elegans daf-2* (DR1572) embryos were added to each well. The plates were incubated for 5 days at 26 °C. Each *B. subtilis* mutant that did not promote animal development was retested on a larger scale using 90 mm plates.

Bacillus genomic DNA extraction and whole genome sequencing – _B. subtilis_

Single bacteria colonies were grown overnight in 3 mL liquid culture. Bacteria culture was centrifuged at 17,000 x g for 1 min. Genomic DNA was isolated as previously described (58). Briefly, the pelleted cells were resuspended in Chromo Lysis Buffer (50 mM EDTA, 0.1M NaCl, pH 7.5). Lysozyme was added (20 µL of 2.5 mg/mL) and incubated at 37 °C for 10 minutes. Sarkosyl was added (1%) and the cells were incubated for 5 minutes at 37 °C. DNA of each isolate was extracted with phenol/chloroform/isoamyl alcohol 25:24:1 and ethanol precipitation. Pelleted were dried and suspended in sterile DI water. Total genomic DNA was quantified using a qubit fluorometer and visualized on a 1% agarose gel for degradation. Genomic DNA from each isolate was submitted for whole genome sequencing on an Illumina platform PE150 at SeqCenter (Pittsburg, PA). FastQC version 0.12.1 (GPL v3) was used to assess the quality control of the raw sequencing data (43). Reads were trimmed using Trimmomatic version 0.39 (44) to remove adapter sequences and low-quality reads (Q<30). Unicycler version v0.5.0 with default parameters was used to assemble the bacterial genome (45).

EMS mutagenesis of WT _C. elegans_

L4 staged WT *C. elegans* were washed in M9 buffer (recipe: 3 g/L KH_2PO_4, 6 g/L Na_2HPO_4, 5 g/L NaCl, 1 mM $MgSO_4$) 3 times and resuspended in 4 mL M9 buffer. 20 µL of Ethyl methanesulfonate (EMS) (Sigma Aldrich, M0880) were added and the animals were incubated for 4 hours with a rotary mixer, at 20 °C. The animals were washed three times and plated in 20

pools of ~200 on *E. coli* OP50 seeded NGM. The animals were screened on *B. subtilis* Δ*speB* for development beyond L4. Approximately one animal from each pool that developed beyond L4 was isolated and whole genome sequenced.

C. elegans genomic DNA extraction and whole genome sequencing

WT *C. elegans* were incubated on NGM for 3 days at 20 °C. The animals were washed in M9 buffer. and suspended 1:1 in Worm Lysis Buffer (50 mM KCl, 10 mM Tris (pH 8.3), 2.5 mM MgCl2, 0.45% Tween 20, 0.01% Gelatin, 0.45% Nonidet P 40 Substitute (Sigma Aldrich, 74385). The animals were incubated at 56 °C for 1 hour with 10 µL of proteinase K (20 mg/mL). After lysis, genomic DNA was purified by phenol chloroform extraction and ethanol precipitation. DNA pellets were resuspended in sterile DI water.

Whole genome Illumina sequencing and variant calling was performed by SeqCenter (Pittsburg, PA). Briefly, Illumina sequencing libraries were prepared using the tagmentation-based and PCR-based Illumina DNA Prep kit and custom IDT 10bp unique dual indices (UDI) with a target insert size of 320 bp. No additional DNA fragmentation or size selection steps were performed. Illumina sequencing was performed on an Illumina NovaSeq 6000 sequencer in one or more multiplexed shared-flow-cell runs, producing 2x151bp paired-end reads. Demultiplexing, quality control and adapter trimming was performed with bcl-convert1 (v4.1.5)" "The fastq paired end reads were prepared for variant calling using Samtools and then indexed using bwa-mem index. Raw reads were then mapped to the indexed reference using bwa-mem and subsequently sorted and converted to BAM files using Samtools. GATK's3 MarkDuplicates functionality was used to remove duplicate reads from the alignment file. GATK's Haplotype caller was then used to call variants on the alignment file. BcfTools was used to filter out variants with a QD < 2, or MQ < 40 or MQRankSum < -12.5, or ReadPosRankSum < -8, or FS > 60.0, or SOR >3.

Microscopy

C. elegans strains were washed with M9 buffer prior to imaging to remove excess bacteria. The animals were paralyzed with tetramisole and incubated for ~2 minutes. Images were taken with a Leica DM6 B upright microscope. Images were pseudo-colored using FIJI (46). Images were assembled in Adobe Illustrator 2024 28.4.1 64-bit (47).

16S rRNA sequencing – Bacillus

To determine an evolutionary relationship among members of *Bacillus* genus that influence animal development, the strains were submitted for Sanger sequencing at Genewiz (South Plainfield, NJ). Consensus sequences of the full-length 16S rRNA were concatenated in a single fasta file. Sequence alignment was performed with MAFFT v7.520 (48). Alignment trimming was performed with trimAl v1.4 (49). A maximum-likelihood-based phylogenetic tree was built with IQ-TREE version 1.6.12 (50). ModelFinder version (-m TEST option) (51) was used to select the best model for the phylogenetic tree construction. Branch support was assessed using 1,000 ultrafast bootstrap approximations (-bb 1000 option) (52). Phylogenetic tree was edited with iTOLs version 6.8.2 (53). The strain *Lactobacillus acidophilus* La-14 (ASM38967v2) was used as a root.

Metabolomics

Metabolites from LB broth were extracted via the addition of ice cold 2:2:1 (v/v) mixture of acetonitrile:methanol:water (#A456, #A955, #W6, respectively; Thermo Fisher Scientific) at a ratio of 30 µl sample per mL of extraction solvent. The samples were vortexed for 10 sec, sonicated for 5 minutes in a water bath sonicator, and incubated on wet ice for 60 min. After incubation, samples were centrifuged at 17,000g and 4 °C to pellet the insoluble fraction. The metabolite-containing supernatant was collected, dried in a vacuum evaporator, and stored at -80°C until derivatization.

Carbamylated-derivatives were generated by derivatizing the dried metabolite fraction with isobutylchloroformate**.** Dried metabolite extracts were resuspended in 200 µL of water containing 1 µg/mL of 1,6 Diaminohexane as an internal standard. 5 µL of sodium bicarbonate (1M, pH 9.0) was added to each sample vial followed by the addition 20 µL of isobutyl chloroformate (177989, Sigma). Samples were vortexed for 10 seconds then incubated at 37 °C for 15 minutes. After cooling to room temperature for 15 minutes, 1 mL of diethyl ether (309966, Sigma) was added, and samples were vortexed for 10 seconds. Samples were then centrifuged for 1 minute to separate the organic and aqueous layers. 800 µL of the carbamylated metabolite containing organic layer was transferred to an autosampler vial, and subsequently dried under a gentle stream of nitrogen gas. Dried samples were resuspended in 100 µL of 1:1 (v/v) acetonitrile:water, vortexed, and 90 µL transferred to a fresh autosampler vial for LC-MS analysis. For LCMS analysis of N1-aminopropylagmatine, chemical standard (EN300-47248193, Enamine) was prepared at 2µg/mL in water and derivatized as described above as either a neat standard or spiked into dried metabolite extracts.

LC-MS analysis was performed on derivatized metabolite extracts analyzed by high resolution accurate mass spectrometry using an ID-X Orbitrap mass spectrometer (Thermo Fisher Scientific) coupled to a Thermo Vanquish Horizon liquid chromatography system. 2 µL of sample volume was injected on column. Chromatographic separations were accomplished with a Cortecs T3 (120Å, 1.6 µm, 2.1 mm × 150 mm) analytical column (#186008500, Waters, Eschborn, Germany) fitted with a pre-guard column (120Å, 1.6 µm, 2.1mm × 5 mm; #186008508, Waters, Eschborn, Germany) using an elution gradient with a binary solvent system. Solvent A consisted of LC/MS grade water (W6–4, Fisher), and Solvent B was 99% LC-MS grade acetonitrile (A955, Fisher). Both mobile phases contained 0.1% (v/v) formic acid (A11710X1, Fisher). The 15-min analytical gradient at a flow rate of 400 µL/min was: 0–0.5 min hold at 100% A, 0.5–2.0 min ramp from 0% B to 40% B, 2.0-10.0 min from 40% B to 99% B,

then held at 99% B from 10.0-15.0 min. Following the analytical separation, the column was re-equilibrated for 3.5 min as follows: 0–0.5 min hold at 100% A at 600 µL/min, 0.5–0.6 min decrease from 600 µL/min to 400 µL/min, 0.6–3.5 min hold at 100% A and 400 µL/min. The column temperature was maintained at 50°C. The H-ESI source was operated at spray voltage of 2500 V(negative mode)/3500 V(positive mode), sheath gas: 70 a.u., aux gas: 25 a.u., sweep gas: 1 a.u., ion transfer tube: 300°C, vaporizer: 250 °C. Sample data were collected via data dependent MS2 (ddMS2) fragmentation using MS1 resolution at 60,000, MS2 resolution at 7,500, intensity threshold at 2.0 × 104, and dynamic exclusion after two triggers for 10 s. MS2 fragmentation was completed first with HCD using stepped collision energies at 15, 30, and 45% and was followed on the next scan by CID fragmentation in assisted collision energy mode at 15, 30, and 45% with an activation Q of 0.25. MS1 scans used custom AGC target of 25% in positive mode and a maximum injection time of 50 ms. MS2 scans used standard AGC target and a maximum injection time of 22ms. The total cycle time of the MS1 and ddMS2 scans was 0.6 s. Untargeted metabolomics data were analyzed in Compound Discoverer (v 3.3, Thermo).

Brood size count

Pristionchus pacificus PS312 grew to adulthood on NGM plates seeded with *E. coli* OP50 at 20 °C. Embryos were isolated using egg preparation solution and plated on NGMB plates seeded with the respective bacterial strains. Bacterial strains were grown overnight at 30 °C before seeding. Once the animals reached the L4 growth stage, 10 animals were singled onto NGMB seeded with the respective bacterial strains, prepared from overnight cultures grown at 30 °C. The plates were incubated at 20 °C for the duration of the experiment. Offspring were counted each day for approximately 5 days. Animals that died on day 1 or 2 were removed from the data set.

References

1. Fleming A. Classics in infectious diseases: on the antibacterial action of cultures of a penicillium, with special reference to their use in the isolation of B. influenzae by Alexander Fleming, Reprinted from the British Journal of Experimental Pathology 10:226-236, 1929. Rev Infect Dis. 1980;2(1):129–39.

2. Gaynes R. The Discovery of Penicillin—New Insights After More Than 75 Years of Clinical Use. Emerg Infect Dis. 2017 May;23(5):849–53.

3. Dubos RJ. STUDIES ON A BACTERICIDAL AGENT EXTRACTED FROM A SOIL BACILLUS : I. PREPARATION OF THE AGENT. ITS ACTIVITY IN VITRO. J Exp Med. 1939 Jun 30;70(1):1–10.

4. Dubos RJ. STUDIES ON A BACTERICIDAL AGENT EXTRACTED FROM A SOIL BACILLUS : II. PROTECTIVE EFFECT OF THE BACTERICIDAL AGENT AGAINST EXPERIMENTAL PNEUMOCOCCUS INFECTIONS IN MICE. J Exp Med. 1939 Jun 30;70(1):11–7.

5. Roesch LFW, Fulthorpe RR, Riva A, Casella G, Hadwin AKM, Kent AD, et al. Pyrosequencing enumerates and contrasts soil microbial diversity. ISME J. 2007 Aug 1;1(4):283–90.

6. Decaëns T, Jiménez JJ, Gioia C, Measey GJ, Lavelle P. The values of soil animals for conservation biology. Eur J Soil Biol. 2006 Nov 1;42:S23–38.

7. Schatz A, Bugle E, Waksman SA. Streptomycin, a Substance Exhibiting Antibiotic Activity Against Gram-Positive and Gram-Negative Bacteria.∗†. Proc Soc Exp Biol Med. 1944 Jan 1;55(1):66–9.

8. Woodruff HB. Selman A. Waksman, Winner of the 1952 Nobel Prize for Physiology or Medicine. Appl Environ Microbiol. 2014 Jan;80(1):2–8.

9. Nielsen UN, Ayres E, Wall DH, Li G, Bardgett RD, Wu T, et al. Global-scale patterns of assemblage structure of soil nematodes in relation to climate and ecosystem properties. Glob Ecol Biogeogr. 2014;23(9):968–78.

10. Kumar A, Baruah A, Tomioka M, Iino Y, Kalita MC, Khan M. Caenorhabditis elegans: a model to understand host–microbe interactions. Cell Mol Life Sci. 2020 Apr 1;77(7):1229–49.

11. CAMPBELL WC, BURG RW, FISHER MH, DYBAS RA. The Discovery of Ivermectin and Other Avermectins. In: Pesticide Synthesis Through Rational Approaches [Internet]. American Chemical Society; 1984 [cited 2024 Apr 2]. p. 5–20. (ACS Symposium Series; vol. 255). Available from: https://doi.org/10.1021/bk-1984-0255.ch001

12. Paghdal KV, Schwartz RA. Sirolimus (rapamycin): From the soil of Easter Island to a bright future. J Am Acad Dermatol. 2007 Dec 1;57(6):1046–50.

13. Lawley TD, Walker AW. Intestinal colonization resistance. Immunology. 2013;138(1):1–11.

14. Nicklas W, Keubler L, Bleich A. Maintaining and Monitoring the Defined Microbiota Status of Gnotobiotic Rodents. ILAR J. 2015 Aug 31;56(2):241–9.

15. Fontaine CA, Skorupski AM, Vowles CJ, Anderson NE, Poe SA, Eaton KA. How free of germs is germ-free? Detection of bacterial contamination in a germ free mouse unit. Gut Microbes. 2015 Jul 4;6(4):225–33.

16. Hu PJ. Dauer. WormBook [Internet]. 2007 [cited 2024 Apr 17]; Available from: http://www.wormbook.org/chapters/www_dauer/dauer.html

17. Koo BM, Kritikos G, Farelli JD, Todor H, Tong K, Kimsey H, et al. Construction and Analysis of Two Genome-Scale Deletion Libraries for Bacillus subtilis. Cell Syst. 2017 Mar;4(3):291-305.e7.

18. Hu PJ. Microbiome: Insulin signaling shapes gut community composition. Curr Biol. 2021 Jun 21;31(12):R803–6.

19. Zhang F, Weckhorst JL, Assié A, Hosea C, Ayoub CA, Khodakova AS, et al. Natural genetic variation drives microbiome selection in the Caenorhabditis elegans gut. Curr Biol. 2021 Jun 21;31(12):2603-2618.e9.

20. Antebi A, Yeh WH, Tait D, Hedgecock EM, Riddle DL. daf-12 encodes a nuclear receptor that regulates the dauer diapause and developmental age in C. elegans. Genes Dev. 2000;14(12):1512–27.

21. Dirksen P, Assié A, Zimmermann J, Zhang F, Tietje AM, Marsh SA, et al. CeMbio - The Caenorhabditis elegans Microbiome Resource. G3 GenesGenomesGenetics. 2020 Sep 1;10(9):3025–39.

22. Sekowska A, Bertin P, Danchin A. Characterization of polyamine synthesis pathway in Bacillus subtilis 168. Mol Microbiol. 1998;29(3):851–8.

23. Sekowska A, Danchin A, Risler JL. Phylogeny of related functions: the case of polyamine biosynthetic enzymes. Microbiology. 2000 Aug 1;146(8):1815–28.

24. Heinick A, Urban K, Roth S, Spies D, Nunes F, Phanstiel IV O, et al. Caenorhabditis elegans P5B-type ATPase CATP-5 operates in polyamine transport and is crucial for norspermidine-mediated suppression of RNA interference. FASEB J. 2010;24(1):206–17.

25. Ohnuma M, Terui Y, Tamakoshi M, Mitome H, Niitsu M, Samejima K, et al. N1-Aminopropylagmatine, a New Polyamine Produced as a Key Intermediate in Polyamine Biosynthesis of an Extreme Thermophile, Thermus thermophilus *. J Biol Chem. 2005 Aug 26;280(34):30073–82.

26. Pellegrino MW, Nargund AM, Kirienko NV, Gillis R, Fiorese CJ, Haynes CM. Mitochondrial UPR-regulated innate immunity provides resistance to pathogen infection. Nature. 2014 Dec;516(7531):414–7.

27. Prabh N, Roeseler W, Witte H, Eberhardt G, Sommer RJ, Rödelsperger C. Deep taxon sampling reveals the evolutionary dynamics of novel gene families in Pristionchus nematodes. Genome Res. 2018 Nov 1;28(11):1664–74.

28. Rödelsperger C, Röseler W, Prabh N, Yoshida K, Weiler C, Herrmann M, et al. Phylotranscriptomics of Pristionchus Nematodes Reveals Parallel Gene Loss in Six Hermaphroditic Lineages. Curr Biol. 2018 Oct;28(19):3123-3127.e5.

29. Han B, Sivaramakrishnan P, Lin CCJ, Neve IAA, He J, Tay LWR, et al. Microbial Genetic Composition Tunes Host Longevity. Cell. 2017 Jun 15;169(7):1249-1262.e13.

30. Lin CCJ, Wang MC. Microbial metabolites regulate host lipid metabolism through NR5A–Hedgehog signalling. Nat Cell Biol. 2017 May;19(5):550–7.

31. Watson E, MacNeil LT, Ritter AD, Yilmaz LS, Rosebrock AP, Caudy AA, et al. Interspecies Systems Biology Uncovers Metabolites Affecting C. elegans Gene Expression and Life History Traits. Cell. 2014 Feb 13;156(4):759–70.

32. MacNeil LT, Watson E, Arda HE, Zhu LJ, Walhout AJM. Diet-Induced Developmental Acceleration Independent of TOR and Insulin in C. elegans. Cell. 2013 Mar 28;153(1):240–52.

33. Samuel BS, Rowedder H, Braendle C, Félix MA, Ruvkun G. Caenorhabditis elegans responses to bacteria from its natural habitats. Proc Natl Acad Sci. 2016 Jul 5;113(27):E3941–9.

34. O'Donnell MP, Fox BW, Chao PH, Schroeder FC, Sengupta P. A neurotransmitter produced by gut bacteria modulates host sensory behaviour. Nature. 2020 Jul;583(7816):415–20.

35. Berg M, Monnin D, Cho J, Nelson L, Crits-Christoph A, Shapira M. TGFβ/BMP immune signaling affects abundance and function of C. elegans gut commensals. Nat Commun. 2019 Feb 5;10(1):604.

36. Kissoyan KAB, Peters L, Giez C, Michels J, Pees B, Hamerich IK, et al. Exploring Effects of C. elegans Protective Natural Microbiota on Host Physiology. Front Cell Infect Microbiol. 2022 Feb 14;12:775728.

37. Madeo F, Eisenberg T, Pietrocola F, Kroemer G. Spermidine in health and disease. Science. 2018 Jan 26;359(6374):eaan2788.

38. PS312 (strain) - WormBase : Nematode Information Resource [Internet]. [cited 2024 Apr 24]. Available from: https://wormbase.org/species/p_pacificus/strain/WBStrain00047433#03--10

39. N2 (strain) - WormBase : Nematode Information Resource [Internet]. [cited 2024 Apr 24]. Available from: https://wormbase.org/species/c_elegans/strain/WBStrain00000001#03--10

40. DR1572 (strain) - WormBase : Nematode Information Resource [Internet]. [cited 2024 Apr 24]. Available from: https://wormbase.org/species/c_elegans/strain/WBStrain00006381#03--10

41. DR40 (strain) - WormBase : Nematode Information Resource [Internet]. [cited 2024 Apr 24]. Available from: https://wormbase.org/species/c_elegans/strain/WBStrain00006167#03--10

42. IG274 (strain) - WormBase : Nematode Information Resource [Internet]. [cited 2024 Apr 24]. Available from: https://wormbase.org/species/c_elegans/strain/WBStrain00021974#03--10

43. JIN810 (strain) - WormBase : Nematode Information Resource [Internet]. [cited 2024 Apr 24]. Available from: https://wormbase.org/species/c_elegans/strain/WBStrain00047320#03--10

44. LD1171 (strain) - WormBase : Nematode Information Resource [Internet]. [cited 2024 Apr 24]. Available from: https://wormbase.org/species/c_elegans/strain/WBStrain00024128#03--10

45. SJ4058 (strain) - WormBase : Nematode Information Resource [Internet]. [cited 2024 Apr 24]. Available from: https://wormbase.org/species/c_elegans/strain/WBStrain00034066#03--10

46. WE5172 (strain) - WormBase : Nematode Information Resource [Internet]. [cited 2024 Apr 24]. Available from: https://wormbase.org/species/c_elegans/strain/WBStrain00040344#03--10

47. CL2070 (strain) - WormBase : Nematode Information Resource [Internet]. [cited 2024 Apr 24]. Available from: https://wormbase.org/species/c_elegans/strain/WBStrain00005096#03--10

48. CL2166 (strain) - WormBase : Nematode Information Resource [Internet]. [cited 2024 Apr 24]. Available from: https://wormbase.org/species/c_elegans/strain/WBStrain00005102#03--10

49. SJ4005 (strain) - WormBase : Nematode Information Resource [Internet]. [cited 2024 Apr 24]. Available from: https://wormbase.org/species/c_elegans/strain/WBStrain00034065#03--10

50. AU133 (strain) - WormBase : Nematode Information Resource [Internet]. [cited 2024 Apr 24]. Available from: https://wormbase.org/species/c_elegans/strain/WBStrain00000264#03--10

51. CF1553 (strain) - WormBase : Nematode Information Resource [Internet]. [cited 2024 Apr 24]. Available from: https://wormbase.org/species/c_elegans/strain/WBStrain00004861#03--10

52. CY573 (strain) - WormBase : Nematode Information Resource [Internet]. [cited 2024 Apr 24]. Available from: https://wormbase.org/species/c_elegans/strain/WBStrain00005340#03--10

53. GL347 (strain) - WormBase : Nematode Information Resource [Internet]. [cited 2024 Apr 24]. Available from: https://wormbase.org/species/c_elegans/strain/WBStrain00049994#03--10

54. Guérout-Fleury AM, Frandsen N, Stragier P. Plasmids for ectopic integration in Bacillus subtilis. Gene. 1996 Nov 21;180(1–2):57–61.

55. Arnaud M, Chastanet A, Débarbouillé M. New Vector for Efficient Allelic Replacement in Naturally Nontransformable, Low-GC-Content, Gram-Positive Bacteria. Appl Environ Microbiol. 2004 Nov;70(11):6887–91.

56. Karp PD, Billington R, Caspi R, Fulcher CA, Latendresse M, Kothari A, et al. The BioCyc collection of microbial genomes and metabolic pathways. Brief Bioinform. 2019 Jul 19;20(4):1085–93.

57. Korbie DJ, Mattick JS. Touchdown PCR for increased specificity and sensitivity in PCR amplification. Nat Protoc. 2008 Sep;3(9):1452–6.

58. Harwood CR, Cutting SM. Molecular Biological Methods for Bacillus. Wiley; 1991. 618 p.

59. Fiji: an open-source platform for biological-image analysis | Nature Methods [Internet]. [cited 2024 Apr 2]. Available from: https://www.nature.com/articles/nmeth.2019

60. Industry-leading vector graphics software | Adobe Illustrator [Internet]. [cited 2024 Apr 2]. Available from: https://www.adobe.com/products/illustrator/campaign/pricing.html

61. Capella-Gutiérrez S, Silla-Martínez JM, Gabaldón T. trimAl: a tool for automated alignment trimming in large-scale phylogenetic analyses. Bioinforma Oxf Engl. 2009 Aug 1;25(15):1972–3.

62. Nguyen LT, Schmidt HA, von Haeseler A, Minh BQ. IQ-TREE: a fast and effective stochastic algorithm for estimating maximum-likelihood phylogenies. Mol Biol Evol. 2015 Jan;32(1):268–74.

63. ModelFinder: fast model selection for accurate phylogenetic estimates | Nature Methods [Internet]. [cited 2024 Apr 2]. Available from: https://www.nature.com/articles/nmeth.4285

64. Minh BQ, Nguyen MAT, von Haeseler A. Ultrafast Approximation for Phylogenetic Bootstrap. Mol Biol Evol. 2013 May 1;30(5):1188–95.